JOURNAL OF GEOPHYSICAL RESEARCH, VOL. 100, NO. D7, PAGES 14,057–14,076, JULY 20, 1995

Volcanic sulfur dioxide measurements from the total ozone mapping spectrometer instruments

A. J. Krueger,[1] L. S. Walter,[1] P. K. Bhartia,[1] C. C. Schnetzler,[2] N. A. Krotkov,[3] I. Sprod,[4] and G. J. S. Bluth[5]

Abstract. The total ozone mapping spectrometer (TOMS), first flown on the Nimbus 7 satellite, has delivered an unanticipated set of unique information about volcanic plumes because of its contiguous spatial mapping and use of UV wavelengths. The accuracies of TOMS sulfur dioxide retrievals, volcanic plume masses, and eruption totals under low-latitude conditions are evaluated using radiative transfer simulations and error analysis. The retrieval algorithm is a simultaneous solution of the absorption optical depth equations including ozone and sulfur dioxide at the four shortest TOMS wavelengths and an empirical correction based on background condition residuals. The retrieval algorithm reproduces model stratospheric sulfur dioxide plume amounts within ±10% over most central scan angles and moderate solar zenith angles if no aerosols or ash are present. The errors grow to 30% under large solar zenith angle conditions. Volcanic ash and sulfate aerosols in the plume in moderate optical depths (0.3) produce an overestimation of the sulfur dioxide by 15–25% depending on particle size and composition. Retrievals of tropospheric volcanic plumes are affected by the reflectivity of the underlying surface or clouds. The precision of individual TOMS SO_2 soundings is limited by data quantization to ±6 Dobson units. The accuracy is independent of most instrument calibration errors but depends linearly on relative SO_2 absorption cross-section errors at the TOMS wavelengths. Volcanic plume mass estimates are dependent on correction of background offsets integrated over the plume area. The errors vary with plume mass and area, thus are highly individual. In general, they are least for moderate size, compact plumes. Estimates of the total mass of explosively erupted sulfur dioxide depend on extrapolation of a series of daily plume masses backward to the time of the eruption. Errors of 15–30% are not unusual. Effusive eruption total mass estimates are more uncertain due to difficulties in separating new from old sulfur dioxide in daily observations.

Introduction

The perspective afforded by satellite observations has developed, or at least heightened, scientists' appreciation of many global phenomena and their interconnections. One of these phenomena is the frequency of large-scale volcanic eruptions which emplace large quantities of sulfur dioxide (SO_2) into the stratosphere where it oxidizes and combines with water to form sulfuric acid aerosol droplets. The aerosol absorbs solar radiation causing heating in the stratospheric region and net cooling on the Earth's surface, both of which can persist for some time due to the aerosol's long residence time.

Eruptions such as those of Tambora in 1815 [*Self et al.*, 1984] and Laki in 1783 [*Sigurdsson*, 1982] have had dramatic effects on global or regional climate. While events of such magnitude are fortunately rare, sensitive observations can testify to similar effects of eruptions of lesser magnitude. This is important because current concerns about global warming due to the increase in anthropogenic greenhouse gases necessitate reliable climate models with concomitant detailed and accurate global observations. In this sense, the occasional emplacement of an aerosol into the stratosphere by moderate to large-scale volcanic eruptions can insert "noise" into the climate warming "signal" causing difficulty in development and validation of climate models. Alternatively, volcanic eruptions provide transient perturbations to the climate which can be useful in testing climate models. Thus it is important to accurately monitor the amount of SO_2 emplaced into the stratosphere by volcanoes.

The emissions of themselves also raise some interesting volcanological questions. At one time, it was assumed that the magnitude of an eruption, as depicted by the volcano explosivity index (VEI) [*Newhall and Self*, 1982] could be used as a relative measure of the amount of SO_2 generated in an eruption, but this has been shown to be only approximately correct [*Schnetzler et al.*, 1992; *Bluth et al.*, 1993]. The source of the great amounts of this gas generated in some eruptions is a matter of some interest to volcanologists [*Wallace and Gerlach*, 1994] and will require continued accurate measurements.

Monitoring volcanoes and observation of their plumes also serves an important function in disaster mitigation, for example, providing timely information on the occurrence and location of plumes so that aircraft can be warned and/or rerouted. While it is the volcanic particulates or ash that is most hazard-

[1]Earth Sciences Directorate, Goddard Space Flight Center, Greenbelt, Maryland.
[2]Department of Geography, University of Maryland, College Park.
[3]Visiting Scientist Program, USRA, Goddard Space Flight Center, Greenbelt, Maryland.
[4]Hughes STX Corporation, Lanham, Maryland.
[5]Department of Geological Engineering and Sciences, Michigan Technological University, Houghton.

Paper number 95JD01222.
0148-0227/95/95JD-01222$05.00

ous, observation of the SO_2 can be used to differentiate the plume from normal clouds.

The total mass of gaseous emissions in explosive eruptions is notably difficult to measure from the ground or aircraft due to the physical size of the plumes. Nevertheless, information has been gained, especially from smaller eruptions, from correlation spectrometer (COSPEC) instruments which were designed for portable applications in pollution monitoring [*Millan*, 1984]. In these, SO_2 is measured with a correlation spectrometer using diffuse skylight as the light source. COSPEC instruments are often carried on field campaigns by volcanologists concerned with potential explosive eruptions as an increase in SO_2 is often a precursor of such an event. The basic principles and techniques of the COSPEC instrument are described by *Stoiber and Jepsen* [1973]. The COSPEC is operated by aiming it through a sulfur-dioxide-bearing plume; it can be used to traverse an individual plume by a movable platform, either car or plane, or may be placed in a fixed location and scan transects across the emitted plume.

Another ground-based technique for measuring SO_2 uses differential spectral absorption by the gas at a set of near-UV wavelengths. Brewer spectrometers are installed in widespread locations to monitor total ozone and sulfur dioxide by observing the extinction of direct sunlight [*Kerr et al.*, 1980].

No instruments have yet been flown in space specifically to measure volcanic gases. However, fortuitous observations of sulfur dioxide have been made with several instruments. These include the total ozone mapping spectrometer (TOMS) on the Nimbus 7 and Meteor 3 satellites, the solar backscatter ultraviolet (SBUV) instrument on Nimbus 7 and NOAA 9 and 11, and the microwave limb sounder (MLS) on the Upper Atmosphere Research Satellite (UARS). The TOMS has been by far the most prolific because of its ability to make contiguous daytime global maps each day and its 15-year continuous record of volcanism.

The basis for TOMS measurement lies in the differential spectral absorption of ozone in the ultraviolet portion of the spectrum, the same absorption which makes the gas an important filter of solar radiation. During the eruption of El Chichon in 1982 it was found that the sulfur dioxide content of the plume produced a strong absorption at the shortest TOMS wavelengths [*Krueger*, 1983], resulting in incorrect total ozone data. It therefore became necessary to identify SO_2-contaminated observations in the ozone data set.

Krueger [1983] also recognized that independent SO_2 retrievals would, of themselves, be of volcanologic interest. This was underscored by the enormous amount of the gas injected into the atmosphere during the explosive eruption of El Chichon. Subsequently, a program of continued observations of volcanic SO_2 was initiated.

This program has resulted in the observation of SO_2 plumes from over 100 eruptions. Nominal accuracy of total measured SO_2 has been estimated to be 30% [*Krueger et al.*, 1990] but until now, there has been no quantitative evaluation of this estimate. One reason for this lies in the difficulty inherent in validating the space observations using ground measurements of spatially and temporally variable volcanic plumes. Relevant ground observations are rare, but still useful. Under the circumstances, ab initio radiative transfer calculations discussed in this paper may be more significant.

The purpose of this paper is to detail the techniques and algorithms used over the past decade in quantitative determination of volcanic SO_2 using the TOMS instrument and to quantify the errors associated with these determinations. The paper deals with the data collected by Nimbus 7 TOMS from November 1, 1978, to May 9, 1993, and the Meteor 3/TOMS from August 22, 1991, to October 1994. The instruments on these satellites are virtually identical, differing only slightly in calibration; however, the different orbits produce data of different quality.

The paper describes the properties of the TOMS instrument of importance in volcanic observations, the algorithms for discriminating sulfur dioxide from ozone, and the accuracy of the results. This is followed by descriptions of the algorithms for total plume mass and for total eruption mass, with an assessment of the errors. The comparisons of TOMS data with other measurements are presented in a section on validation, and plans for algorithm improvements are briefly described. The discrimination algorithm accuracy has, at present, been evaluated for low-latitude conditions. Nevertheless, the results apply to more than half of all reported eruptions in the TOMS data set and include all of the largest eruptions, such as Pinatubo in 1991 and El Chichon in 1982.

TOMS Instrument Characteristics

A number of spaceborne instruments have been developed to make spectral observations in the near-ultraviolet portion of the spectrum, primarily for the purpose of measuring ozone. The chief instrument for monitoring ozone has been the TOMS. Although not able to measure the concentration of ozone as a function of height in the atmosphere, TOMS has the distinct advantage of producing spatially contiguous maps of ozone column amounts.

TOMS is an ultraviolet (UV) spectrophotometer [*Heath et al.*, 1975] which compares the spectral radiance of the sunlit Earth's atmosphere with the radiance of a sunlit-calibrated diffuser plate from a satellite platform. The spectral reflectivity of the atmosphere (sometimes referred to as albedo), which varies with ozone amount and many other geometric and atmospheric parameters, is proportional to the ratio of these two quantities.

The spectrometer is an Ebert configuration which has been modified to select six wavelengths by means of multiple exit slits. The wavelength bands are individually selected by a chopper wheel for multiplexing at a photomultiplier detector. Six fixed wavelength bands in the 312- to 380-nm region were chosen for the measurement of total ozone by differential absorption in the near-UV Huggins bands of ozone. The wavelengths are used in two pairs which are sensitive to ozone changes at all solar zenith angles. In addition, the contribution of ground or clouds to the radiance is measured at two longer, unabsorbed wavelengths.

The TOMS band-averaged absorption spectra of ozone over the range 300–340 nm from *Bass and Paur* [1984], and sulfur dioxide in the range 300–320 nm from *McGee and Burris* [1987], and 320–340 nm from *Wu and Judge* [1981] are shown in Figure 1. Ozone has a nearly exponential absorption spectrum which becomes banded at wavelengths longer than 320 nm, while sulfur dioxide has large amplitude bands throughout its spectrum. SO_2 is the stronger absorber at short wavelengths, but it dies out more rapidly than ozone beyond 320 nm. It is the differences in the absorption coefficients at the TOMS wavelengths which are important in discrimination between the two species. The shortest four TOMS wavelengths are indicated on Figure 1 by the dashed vertical lines. These wavelengths, the band-weighted (or effective) ozone and sulfur dioxide absorp-

tion coefficients, and the ratio of sulfur dioxide to ozone absorption coefficients in the TOMS data production algorithm are listed in Table 1. The SO_2 absorption coefficients are based on *Wu and Judge* [1981] measurements at room temperature (294 K). These coefficients are in units of atmosphere centimeter (atm cm)$^{-1}$, the extinction per centimeter thickness of gas under standard temperature-pressure conditions. Total ozone is usually measured in atm cm; for convenience the amount is multiplied by 1000 and referred to as "Dobson units" or "DU." We have elected to specify total sulfur dioxide in these units.

The TOMS instrument is designed to produce contiguous global mapping and daily coverage so that transient, small features, such as perturbations in the ozone near upper air fronts, can be observed. This is accomplished by providing the sensor with a scan mirror to direct the field of view in cross-track positions, thus creating traces which run parallel to the nadir trace. The TOMS was optimized for the Nimbus 7 case; a 955-km circular, 99.28° inclination, Sun-synchronous noon-midnight orbit. The instantaneous field of view is 3° × 3°, which results in a 50 × 50 km ground footprint at nadir from the Nimbus altitude; contiguous coverage between orbits is obtained by the scan mirror which is directed in thirty-five 3° scan steps to produce a 3000-km-wide swath. Contiguous coverage along the flight track is obtained by making one scan each 8 s, the time for the subsatellite point to move 50 km. This is illustrated in the top of Figure 2, where the footprints of each of the 35 scenes are shown for two scans as a function of cross-track distance. The diamond-shaped patterns are produced by the projection of the square field of view (FOV) on the surface of the Earth after rotation by the scan mirror.

The footprint area as a function of scan position is shown at the bottom of Figure 2 (left scale). The nadir (scan position 18) area is 2500 km^2 from the Nimbus altitude. This area remains within a factor of 2 of the nadir footprint for the 23 scan positions bracketing nadir; at the largest scan position (51°) the footprint grows to 7.6 times larger than the nadir footprint. This has an effect on the resolution of ozone features at the edge of the swath and on the minimum size sulfur dioxide plume that can be detected. The number of metric tons of sulfur dioxide within each footprint for each 1 DU of sulfur dioxide is shown by the right-hand scale as a function of scan position. This ranges from 71 at nadir to 540 at the edge of the swath.

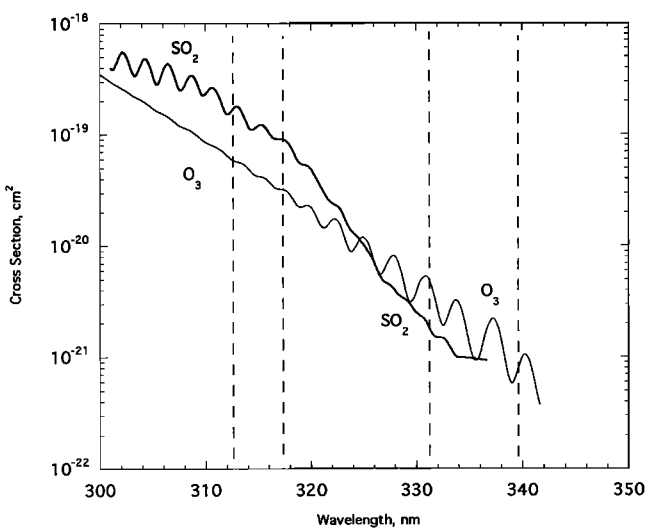

Figure 1. The low temperature (210 K) absorption spectra of ozone and sulfur dioxide smoothed by the 1.1-nm band pass of TOMS over the 300- to 320-nm spectral range. Room temperature SO_2 data are shown for 320–340 nm.

Table 1. TOMS Effective Absorption Coefficients

Wavelength, nm	SO_2 Absorption Coefficient, (atm cm^{-1})	O_3 Absorption Coefficient, (atm cm^{-1})	SO_2/O_3 Absorption Coefficient Ratio
312.5	4.2	1.651	2.54
317.5	2.35	0.886	2.65
331.2	0.046	0.147	0.313
339.8	0.018	0.027	0.667

TOMS, total ozone mapping spectrometer.

At the TOMS wavelengths the albedo is strongly influenced by meteorological clouds. At small solar zenith angles the scene radiance changes by more than a factor of 4 between clear and cloudy scenes. TOMS is designed to avoid biases due to image motion by sampling each of the six wavelengths 4 times during the 0.2-s dwell time at each scene.

Ozone and Sulfur Dioxide Discrimination

The algorithm for retrieving total ozone from TOMS data depends on theoretical calculations of backscattered radiances using a multiple-scattering radiative transfer model [*Dave and Mateer*, 1967]. The albedo at each wavelength is precomputed for the entire range of geophysical and geometrical observing conditions encountered by the satellite. Among the geophysical parameters is the average vertical distribution of ozone for different latitude zones and total ozone amounts. Two pairs of wavelengths are used to minimize modeling errors to permit accurate ozone estimates over a factor of 4 change in slant ozone amount (ozone amount times geometric path) from tropics to high latitudes.

Like ozone, sulfur dioxide gas is a strong absorber of UV radiation. Typically, the amount of sulfur dioxide in the region of the atmosphere that affects TOMS-measured radiances (above the boundary layer) is too small to cause significant absorption. However, a volcanic eruption can produce enough SO_2 in a localized region to produce UV absorption comparable to or even exceeding the ozone absorption at the shortest two TOMS wavelengths. In such cases the present TOMS algorithm incorrectly interprets SO_2 as enhanced ozone. The problem is to discriminate between sulfur dioxide and ozone using either spatial or spectral information.

Two methods have been used to compute sulfur dioxide column amounts from TOMS data. A "residual" model was employed by *Krueger* [1983] to demonstrate that absorption within volcanic clouds was due to sulfur dioxide. Limitations of this method were alleviated with a new "linear" model, which is currently used for eruption analysis.

Residual Model

The first observation of the UV albedo of volcanic plumes was made with the Nimbus 7 TOMS during the eruption of El Chichon in 1982 [*Krueger*, 1983]. The plume was observed to absorb strongly at the shortest two TOMS wavelengths but was almost undetectable at the other wavelengths. This signature was consistent with sulfur dioxide absorption within the plume. Sulfur dioxide column amounts were estimated by assuming

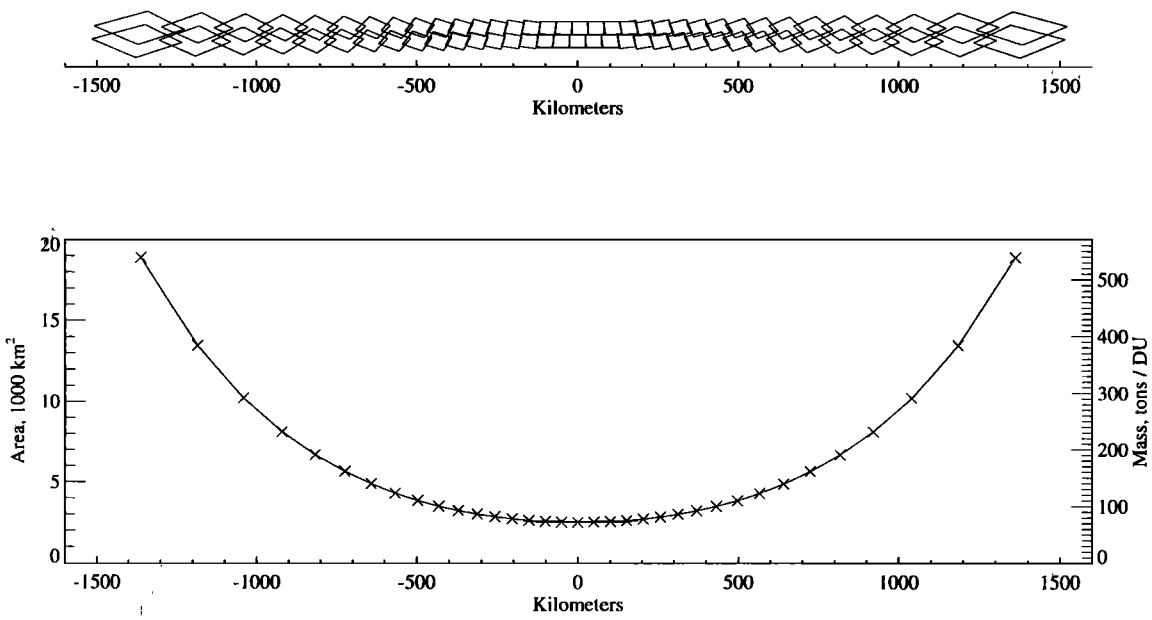

Figure 2. Total ozone mapping spectrometer (TOMS) footprints. The top chart shows the footprints corresponding to the 35 scan positions of the Nimbus 7 TOMS for two adjacent scans. On the bottom chart, the footprint area and the mass of sulfur dioxide in each footprint in tons per Dobson unit (DU) total SO_2 are shown as functions of distance from nadir. Each scan position is indicated by a cross on the bottom panel.

that changes from the background albedo at individual absorbed wavelengths were due solely to absorption by SO_2. The background albedo was estimated by interpolating between plume-free areas south and north of the plume assuming that the ozone is undisturbed within the plume. Ash particles and aerosols, which are expected to have a much broader spectral signature than sulfur dioxide, appeared to have no effect because of the lack of albedo changes at the longer, nonabsorbed wavelengths. Column SO_2 amounts, computed at the two strongly absorbed wavelengths, were in agreement within 10%, lending confidence in the validity of the assumptions.

Linear Model (Kerr Algorithm)

The residual method fails if the background cannot be estimated due to water clouds underlying the volcanic plume. Because this is frequently the case, a more robust algorithm is required for general use. An algorithm used by the Atmospheric Environment Service of Canada to process ground-based observations of ozone and sulfur dioxide column amounts with Brewer spectrophotometer data [*Kerr et al.*, 1980] has been adapted for operational processing of the satellite data. This method makes use of the spectral information obtained by TOMS.

When the direct solar radiation at a wavelength λ is measured from the ground with a Brewer spectrophotometer, the measured flux $F(\lambda)$ is related to the total optical path $\tau(\lambda)$ of the radiation through the atmosphere by Beer's law:

$$F(\lambda) = F_0(\lambda) \exp [-\tau(\lambda)] \quad (1)$$

where F_0 is the extraterrestrial solar flux and τ is the sum of the optical paths of all species.

$$\tau = \tau_{\text{ozone}} + \tau_{\text{sulfur dioxide}} + \tau_{\text{Rayleigh}} + \tau_{\text{aerosol}} \quad (2)$$

The optical path is the product of the attenuation coefficient α, the attenuator amount ξ, and the geometrical path s.

$$\tau = \alpha \xi s \quad (3)$$

If one takes measurements at multiple wavelengths, one has a set of linear equations similar to (3), which can be written in matrix form as

$$[\tau] = [\alpha] [\xi s], \quad (4)$$

where $[\tau]$ and $[\xi s]$ are column matrices and $[\alpha]$ is a square matrix containing the absorption or scattering coefficients. The constituents can be obtained by inverting this equation:

$$[\xi s] = [\alpha]^{-1} [\tau]. \quad (5)$$

In principle, if the wavelength dependence of τ for all attenuating species is known accurately and if these dependencies are sufficiently different from each other, (5) can be used to determine τ for all absorbing and scattering species. However, in practice, the accuracy is limited by the fact that the spectral dependence of τ_{aerosol} is usually not known very accurately.

In applying this technique to TOMS measurements, we make two key assumptions. First, we assume that the solar radiation backscattered to the satellite is attenuated by the absorbing species in a manner similar to (1), that is,

$$I(\lambda) = I_0(\lambda) \exp [-\tau_a(\lambda)] \quad (6)$$

where $I(\lambda)$ is the intensity of the radiation at wavelength λ reaching the satellite, τ_a is the absorption optical path through the atmosphere, and I_0 is the expected intensity in absence of any atmospheric absorption. Second, to solve (6), we need to make an additional assumption about the spectral dependence of I_0. On the basis of radiative transfer calculations, for clear scenes as well as for scenes containing aerosols and clouds, the spectral dependence of $I_0(\lambda)$ over the 27 nm that separates the four shortest wavelengths of TOMS (313–340 nm) can be approximated by

Table 2. Inverse SO_2 Coefficients and Normalized Values Used in Data Processing

Wavelength, λ_i	A_i	A_i, Normalized
312.5	−0.9656	−1
317.5	2.1921	2.270
331.2	−2.6227	−2.716
339.8	1.3963	1.446

$$I_0(\lambda) = aF_0(\lambda) \exp(-b\lambda) \quad (7)$$

where the unknown coefficients a and b vary with measurement geometry and amount of aerosols and clouds in the scene. Combining (6) and (7), one gets a functional form similar to (1)

$$I(\lambda) = aF_0(\lambda) \exp[-b\lambda - \tau_a(\lambda)] \quad (8)$$

Given TOMS-measured N values ($=-100 \log_{10} I/F_0$) at four wavelengths and definition of τ from (3), (8) can be written in matrix form as

$$\begin{bmatrix} N_1 \\ N_2 \\ N_3 \\ N_4 \end{bmatrix} = \begin{bmatrix} 1 & \lambda_1 & \alpha_1 & \alpha'_1 \\ 1 & \lambda_2 & \alpha_2 & \alpha'_2 \\ 1 & \lambda_3 & \alpha_3 & \alpha'_3 \\ 1 & \lambda_4 & \alpha_4 & \alpha'_4 \end{bmatrix} \begin{bmatrix} N_0 \\ kb \\ k\Omega s \\ k\Sigma s \end{bmatrix} \quad (9)$$

where $N_0 = -100 \log_{10}(a)$; $k = 100 \log_{10} e$; Ω is the column ozone; Σ is the column SO_2; $s = \sec\Theta_0 + \sec\Theta$, the geometric path of sunlight entering the atmosphere at solar zenith angle Θ_0 and exiting the atmosphere at the satellite zenith angle Θ; and α and α' are the ozone and sulfur dioxide absorption coefficients (per unit column amount). The SO_2 column amount Σ can be estimated by inverting (9), which has the general form

$$\Sigma = (A_1N_1 + A_2N_2 + A_3N_3 + A_4N_4)/ks \quad (10)$$

The inverse coefficients for SO_2 are given in Table 2, together with the normalized values used in the production code for Nimbus and Meteor 3 TOMS. The production coefficients are scaled by the ratio of DU per atm cm = 1000.

The linear algorithm assumes that absorption optical depth τ is proportional to the observed N values. This relationship has been tested using a radiative transfer model [*Dave*, 1972] to simulate the albedos for a wide variation of the observational conditions encountered by the satellite at low latitudes (N. A. Krotkov et al., manuscript in preparation, 1995 (herein after referred to as K95)). The model results for three low-latitude ozone profiles (225, 275, and 325 DU) and three SO_2 column amounts (0, 50, and 100 DU) under aerosol-free conditions have been plotted together in Figure 3. The results for overhead Sun ($\Theta_0 = 0$) and for satellite zenith angles of 0° and 32° (the central 21 scan positions) are presented for simplicity. These results apply qualitatively to other solar zenith angle (SZA) and satellite zenith angle conditions. It should be noted that total SO_2 values greater than 100 DU in the TOMS database are observed only in the first day of eruptions except for the largest eruptions (Pinatubo, El Chichon). The N values for 312.5 and 317.5 nm are plotted versus absorption optical depth along the geometric path s. The required linear relationship between N and τ is found for both wavelengths (correlation coefficients of 0.9997 and 0.9998) under this wide range of

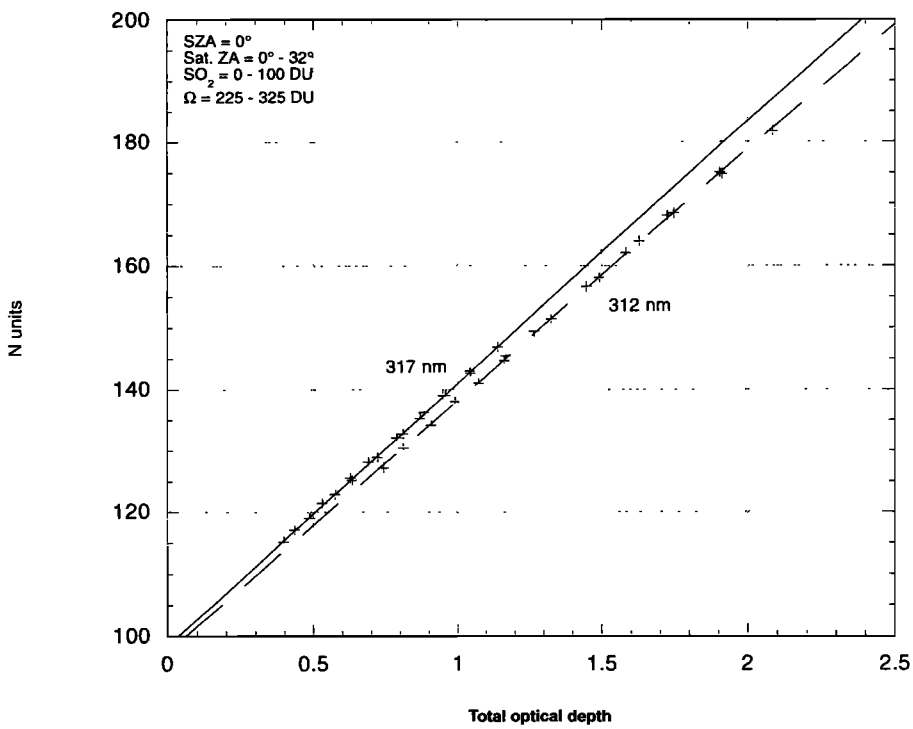

Figure 3. Simulated TOMS N value at 312.5 and 317.5 nm as a function of the atmospheric absorbing optical depth along the geometrical path for solar zenith angle equal to 0° and satellite zenith angles of 0° and 32°. Model results are based on 225, 275, and 325 DU low-latitude ozone profiles and 0, 50, and 100 DU SO_2 column amounts under clear sky conditions (1 atm surface pressure and zero surface reflectivity). The SO_2 layer has a Gaussian vertical distribution with maximum at height 25 km and half width 2 km.

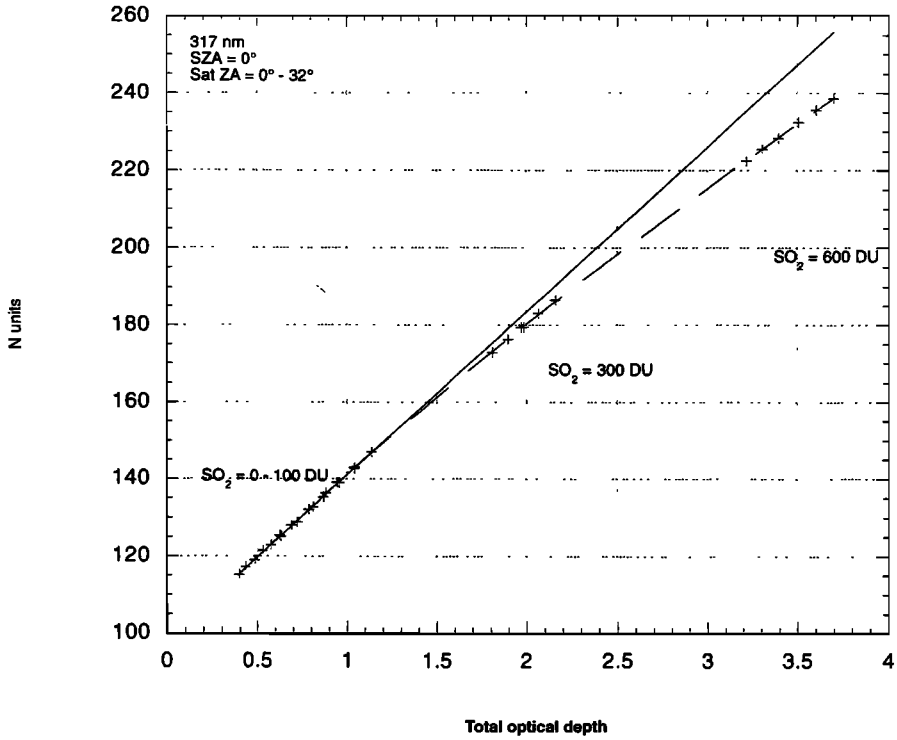

Figure 4. Simulated TOMS N values versus absorbing optical depth for extreme volcanic plume conditions. Conditions are similar to Figure 3 except 317.5 nm only and SO_2 column amounts include 300 and 600 DU. The solid line is the least squares fit to the data of optical depth less than 1.2.

low-latitude conditions. The exact linear relationship depends on wavelength due to Rayleigh cross-section differences.

This relation has also been tested under extreme volcanic plume conditions. Values of 600 DU were found in the Pinatubo plume within 24 hours of the major eruption. Figure 4 illustrates the departure at 317 nm for 300 and 600 DU SO_2 in comparison with the extrapolated linear fit from the 0–100 DU SO_2 conditions. The nonlinearity is even greater at 312 nm, indicating that the geometric path assumption is not valid due to the great absorption within the plume.

Sulfur Dioxide Index (SOI) Algorithm

Background sulfur dioxide concentrations in the stratosphere and troposphere above the polluted boundary layer are generally less than 1 $\mu g\ m^{-3}$ [*Georgii*, 1978]. When integrated through the atmosphere, the total column amount is less than 1 DU, an amount well within the noise level of TOMS SO_2 data. However, the linear algorithm returns background levels which vary by as much as 15 DU as the total ozone and observing path change. A global average empirical correction was computed, in which the false background levels calculated from (10) on a nonvolcanic day were fitted to a quadratic function of slant path times ozone. This corrected value is called the sulfur dioxide index (SOI), which is calculated using the following expression:

$$s\ \mathrm{SOI} = s\Sigma - 11.6 + 66.10\ (s\Omega) - 78.50\ (s\Omega)^2 \qquad (11)$$

where Ω is the apparent total ozone amount in atm cm (DU/1000) derived by the total ozone algorithm described above and s is the geometric path. The SOI values are recorded on the level 2 high-density TOMS (HDTOMS) data tapes which are available through the National Space Science Data Center at Goddard Space Flight Center.

Simulation of SOI Algorithm for Background Conditions

The success of the SOI corrections has been analyzed under background conditions at low latitudes by means of a radiative transfer model. The SO_2 and SOI variations as a function of satellite zenith angle are illustrated in Figure 5 for clear sky and cloudy conditions with 275 DU ozone and without aerosols for two solar zenith angles, $\Theta_0 = 30°$ and 66°. The satellite zenith angle Θ is related to the scan position, $n = 1, \ldots, 35$, for the Nimbus orbit, in the following way:

$$\sin \Theta = ((r+h)/r) \sin [3(n-18)] = 1.15 \sin [3(n-18)], \qquad (12)$$

where r is radius of the Earth and h is satellite height. At low Θ_0 (top), the pure Kerr algorithm (solid curve) has a 5 DU bias at the nadir and a clear scan angle dependence, reaching 10 DU at the edge of the scan. At $\Theta_0 = 66°$, the bias has increased to 8 DU at the nadir and 17 DU at the largest scan angle. This behavior is due to very subtle nonlinearities (<1 N unit) in the N versus τ relationship.

The quadratic correction (dashed curve) works very effectively at large solar angles, removing most of the bias and all of the scan angle dependence. However, at low Θ_0 it fails to correct the nadir offset and overcorrects at the largest scan angles. This is undoubtedly due to the strong influence of large solar zenith angle data in the development of the quadratic correction.

Figure 5 also shows the effect of cloudy conditions on the

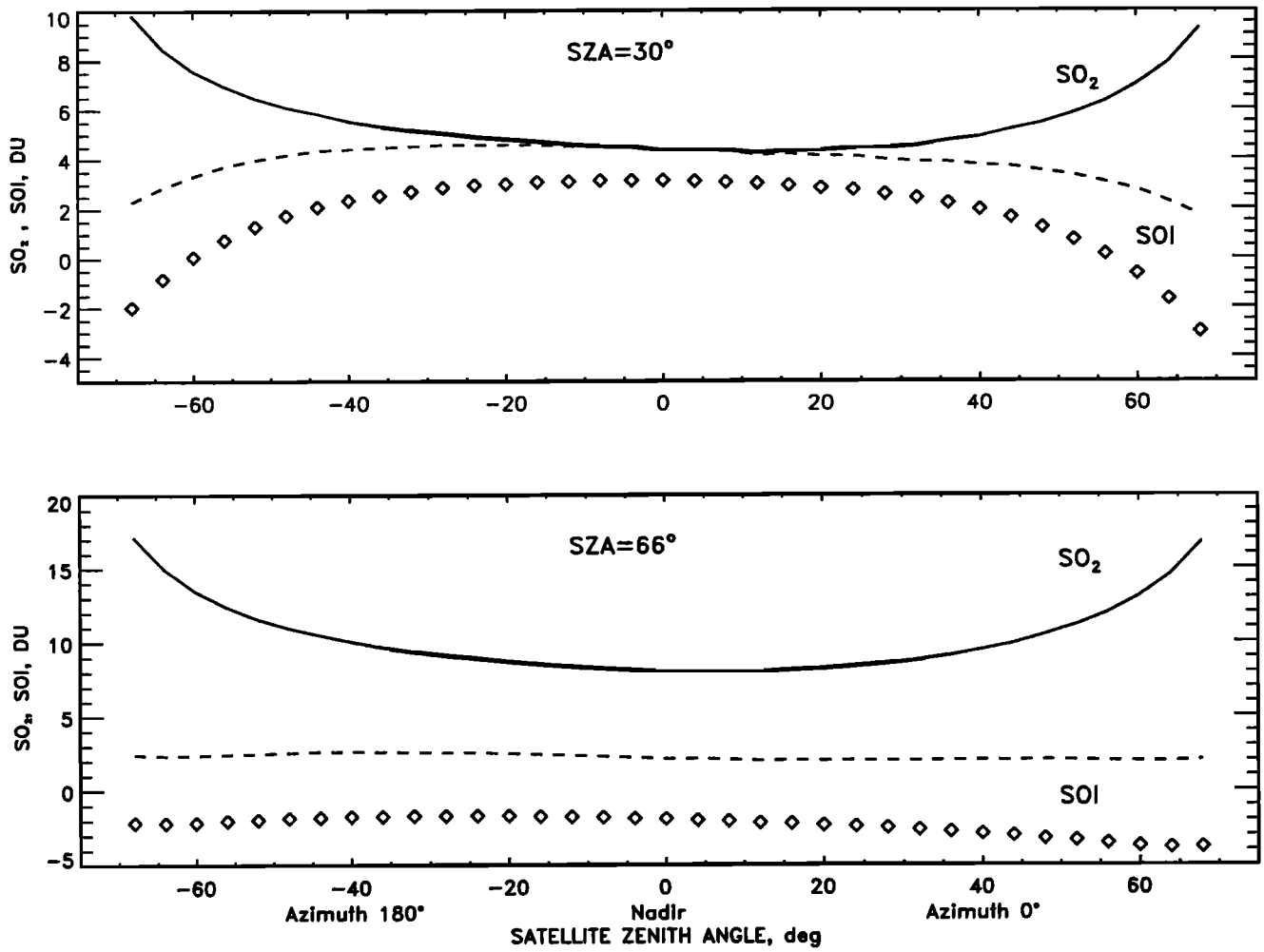

Figure 5. Modeled background SO_2 retrievals as a function of the satellite zenith angle for solar zenith angle equal to 30° (top) and 66° (bottom). Solid curves represent linear model results and dashed lines represent SOI (linear model with quadratic correction applied). Model parameters: clear sky conditions (1 atm surface pressure and zero surface reflectivity) for 275 low-latitude ozone profile. Diamonds show the negatively biased background SOI levels over high, thick meteorological clouds (100-mbar cloud top pressure with 95% reflectivity).

SOI background retrievals. High (p = 100 mbar), dense (R = 95%) clouds were simulated with the radiative transfer model. The SOI was reduced under all conditions by 1–5 DU. This results in negative values for large solar zenith angles and even for small solar zenith angles at the edge of the scan. These results suggest that the quadratic correction could be improved for low-latitude conditions.

These biases are also found in the TOMS data. Figure 12 shows the average measured SOI at each scan position on a nonvolcanic day at tropical latitudes. The appearance is very similar to the model calculations although the TOMS data show a stronger decrease on the left side of the scan, perhaps due to ozone profile and solar zenith angle changes across the swath.

Observed Variations in Background SOI

The average background SOI levels are found to have geophysical variations associated with latitude and season. An example is shown in Figure 6: the zonal mean SOI versus latitude for low-reflectivity (R < 40%) conditions on a volcanic plume-free day, March 17, 1992. In this equinoxial case, reasonably constant SOI levels near 4.5 DU are found over a broad range of latitudes from 60°S to 10°N. However, a distinct dip to 3 DU is found at northern midlatitudes. The southern polar regions show an increase to 7 DU which is not reflected in the northern hemisphere. These features are found to persist for several weeks but are not simply correlated with total ozone, solar zenith angle, or average reflectivity. However, a combination of all three factors might explain this behavior. This pattern evolves with time in a complicated fashion.

Empirical Corrections to Local SOI Values

The observed scan angle background variations noted above produce errors in volcanic plume mass calculations. In addition, meteorological clouds produce larger negative offsets than appear in the simulations. Thus we have developed corrections based on the background data in the vicinity of the volcanic plumes. Figure 7 shows an example of SOI plotted versus TOMS scene reflectivity R measured at 360 and 380 nm from three low-latitude orbit segments. The SOI data (dashed curve) have a nearly constant offset of 5 DU for R < 50%, then decrease more or less linearly with higher reflectivity,

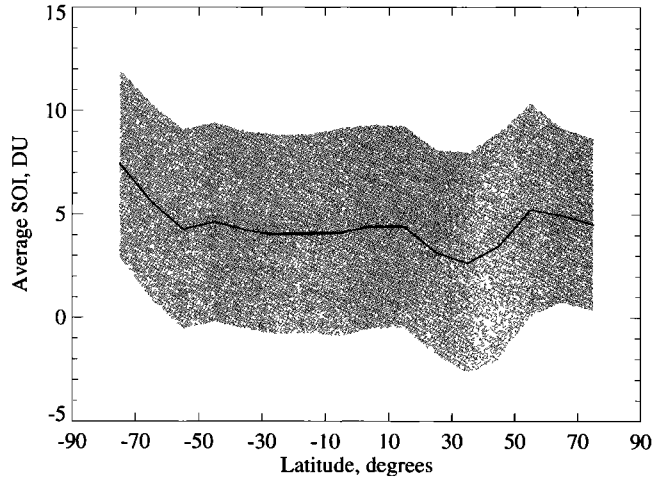

Figure 6. Average (zonal mean) background sulfur dioxide index (SOI) as a function of latitude for March 17, 1992. The ± one standard deviation range of SOI is shaded.

reaching about −10 DU at the highest reflectivities. A linear fit to the high-reflectivity SOI data is used to remove the reflectivity dependence, as shown by the solid curve in Figure 7. We assume that the same offsets apply within the volcanic plume and apply this correction when assessing SO_2 masses. Each volcanic case is analyzed individually, using a reflectivity correction derived in the vicinity of the plume.

The scan angle bias shown in Figure 5 can also affect plume mass estimates. It is visible in images as a "scalloping" effect on both background and volcanic plume areas (e.g., as seen in the Pinatubo plume images in the work of *Bluth et al.* [1992]). This bias is empirically removed by simply calculating the average background SOI at each scan position and then subtracting the correct amount from each TOMS point by scan position. Background SOI levels are found to change with location and time as noted below. Thus the scan angle correction is determined in background areas adjacent to each plume.

Accuracy of SOI Algorithm

In this section we examine the effect of errors due to the instrument, in laboratory data and in related geophysical parameters on the measurement of SO_2 within each footprint. A section below deals with additional errors in aggregation of these footprints for total plume measurements.

Uncertainties in the TOMS radiance measurements and in the albedo calibration of the instrument propagate through the retrieval algorithm to produce uncertainties in the sulfur dioxide amounts. In addition, the absorption cross-section data have errors which can affect the results. Finally, the absorption cross sections are dependent on temperature. In general, we do not have measurements of the temperature within volcanic plumes, although reasonable estimates can be made on the basis of thermodynamic arguments. The Kerr algorithm is surprisingly robust, due to its dependence on contrast between the absorption features of the gases rather than on absolute characteristics. Each of these sources of error are discussed below.

After fixing all of the coefficients in the SOI algorithm we can then test its fidelity with simulated volcanic plume albedo data. The remainder of this section is devoted to a discussion of errors in SO_2 amounts due to geometric and geophysical effects. The effects include solar zenith angle, scan angle, plume altitude, and ash and aerosols within the plume.

Random Measurement Errors

Given σ_N as the 1σ random error in the TOMS N values, the error in computing Σ using (10) and (11) is given by

$$ks\sigma_\Sigma = k\sigma_N\{A_1^2 + A_2^2 + A_3^2 + A_4^2\}^{1/2} = 91\sigma_N \qquad (13)$$

Using the estimated 0.3% quantization and measurement errors in TOMS radiances, $\sigma_N = 0.13$, giving $ks\sigma_\Sigma = 11.8$. The maximum error in Σ of 5.9 DU is obtained when s is equal to 2 but will decrease from this value in proportion to s.

However, the error in computing the SOI from (11) includes both measurement errors and errors in the quadratic correction. Figure 8 shows a histogram of the SOI values from TOMS data taken on a nonvolcanic day. The standard deviation at nadir ($\sigma_{SOI} = 5.7$ DU) is in good agreement with values computed from (13) at small solar zenith angles. This indicates that the geophysical background noise is not a significant contributor to the total noise. At the edge of the scan ($s = 3.88$ for overhead Sun), the predicted noise, $\sigma_\Sigma = 3.0$ DU, is less than the observed noise, $\sigma_{SOI} = 4.4$ DU. This is because the background noise increases with $s\Omega$, as the magnitude of the correction itself increases. Since the background correction is an artifact of the assumptions made in deriving (10), and is not a fundamental error like the measurement noise, there appears to be some room for noise reduction at large solar zenith angles by using a better SO_2 discrimination algorithm.

Instrument Calibration Errors

From the properties of the matrix in (9) as well as from the calculated coefficients given in (11), one can easily show that the computation of Σ is not affected either by a constant wavelength independent error in all N values (equivalent to a constant percentage error in measuring I/F_0) or by an error that is exactly linear with wavelength. It turns out that these errors are the most likely type of errors one has in estimating the N values from the TOMS measurements. Moreover, from (10), calibration errors that vary with wavelength in a complicated

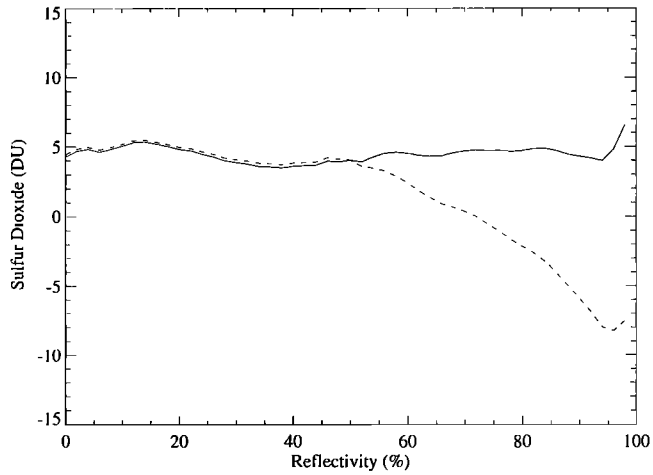

Figure 7. Observed background sulfur dioxide levels as a function of reflectivity. The SOI values are independent of reflectivity when $R < 50\%$ but decrease almost linearly at higher reflectances, as shown by the dashed curve. The solid curve shows the result of correction by a linear fit of the $R > 50\%$ data.

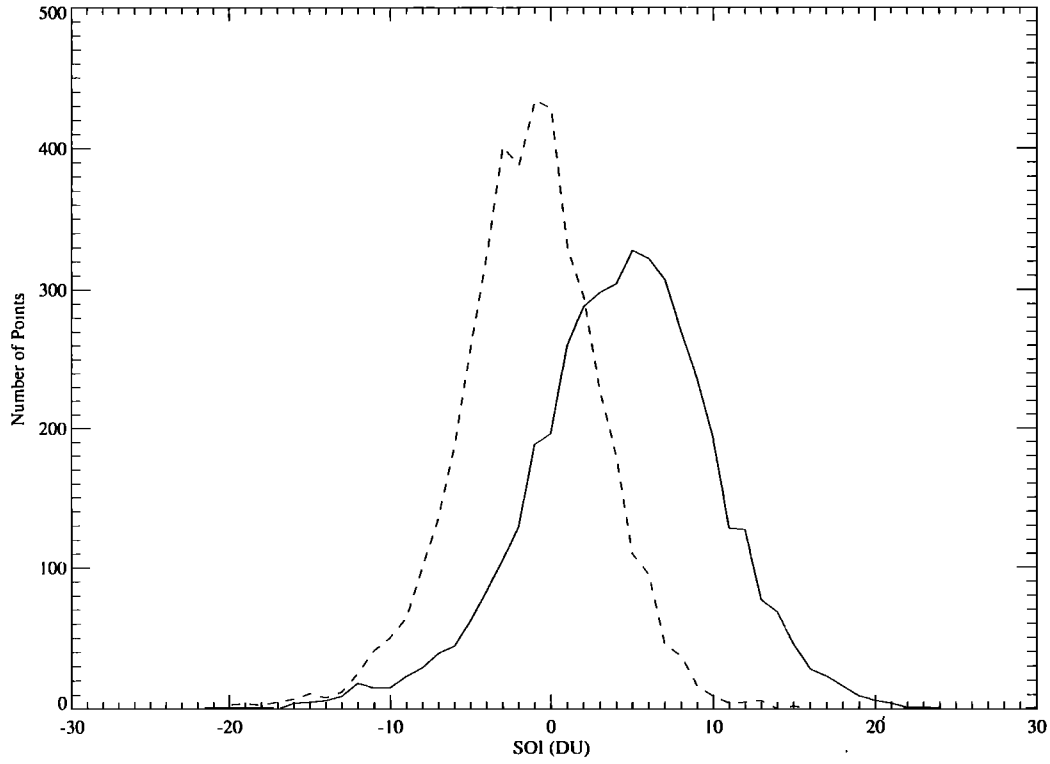

Figure 8. Histograms of background SOI data at one scan edge, position 1 (dashed curve) and at nadir (solid curve). The average and standard deviation of the SOI values at the scan edge (-1.4 ± 4.4 DU) are lower than at nadir (4.3 ± 5.7 DU).

way would simply introduce a constant background value which would be subtracted out in computing SOI from (12). Therefore instrument calibration errors do not contribute to the overall error budget.

Cross-Section Errors

The linear algorithm results are biased by errors in the effective absorption coefficients. The sensitivity to these errors depends on differences between the ozone and the sulfur dioxide coefficients. In principle, the instrument wavelengths are chosen to maximize the "contrast" between the absorbers. However, the TOMS wavelengths were selected for total ozone determination without regard of sulfur dioxide, which was at that time (1967) not known to be present in the atmosphere in significant amounts.

The propagation of absorption coefficient errors is given as follows: The ratio of the fractional deviation of the sulfur dioxide amount to the fractional error in absorption coefficient at a given wavelength is

$$(\Sigma'/\Sigma)/(\alpha_i'/\alpha_i) = -A_i\alpha_i \qquad (14)$$

where Σ' and Σ are the perturbed and normal sulfur dioxide amounts and α_i' and α_i are the perturbed and normal absorption coefficients at the ith wavelength, respectively, and A_i is the inverted coefficient for that wavelength. The sensitivity of the retrieved SO_2 to 1% errors in the sulfur dioxide coefficients are shown in column 4 of Table 3. This table indicates that a 1% error in the absorption coefficient at 312.5 nm will produce a 4.0% error in sulfur dioxide column amount. These errors, however, will be compensated if the 317.5-nm absorption coefficients are also biased in the same direction. Thus the sulfur dioxide retrievals are nearly insensitive to constant biases in the absorption coefficient data. However, random errors in the absorption coefficient data can produce significant biases in the retrievals. *McGee and Burris* [1987] report relative measurement errors at the 312- and 317-nm spectral regions of 2 and 3%, respectively, with a 0.03-nm spectral resolution. The precision of slit-averaged effective absorption coefficients with 1-nm bandwidth would be improved by $1/\sqrt{}$(number of samples), or 0.36 and 0.55% for these two spectral regions, leading to 1.5 and 2.8% errors in sulfur dioxide retrievals, for a worst case error of 4.3%.

The sulfur dioxide UV absorption spectrum is temperature dependent. The temperature coefficients at the 312- and 317-nm TOMS bands are 0.07 and 0.10%/K, respectively [*McGee and Burris*, 1987], based on a linear fit of the cross sections at 210 and 295 K. The coefficients are of the same sign, so that they tend to compensate in the sulfur dioxide retrieval. Thus for a 20°K error in plume temperature the retrieval error would be 20 (0.07 − 0.10) = −0.6%. The temperature coeffi-

Table 3. Percentage Error in Sulfur Dioxide Produced by 1% Errors in the Effective Absorption Coefficients for TOMS Wavelengths

Wavelength	A_i	α_i SO_2	Error Factor
312.5	−0.9656	4.2	4.05
317.5	2.1921	2.35	−5.15
331.2	−2.6227	0.046	0.12
339.8	1.3963	0.018	−0.02

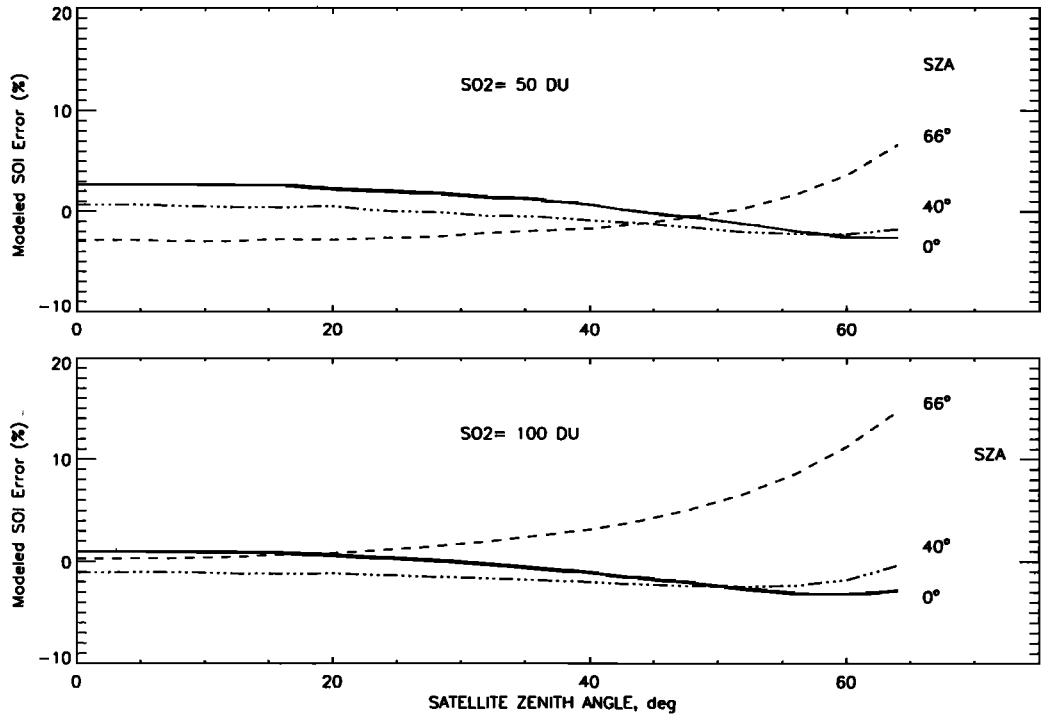

Figure 9. Simulated TOMS SO_2 error as a function of the satellite vertical angle for solar zenith angles equal to 0° (solid curve), 40° (dotted-dashed curve) and 66° (dashed). The SO_2 column amounts are 50 DU (top) and 100 DU (bottom). Other model conditions: The SO_2 plume is at 25 km altitude in a 275-DU low-latitude ozone profile with clear sky, no-aerosol conditions, satellite azimuth angle is 90°.

cients vary with wavelength so that these results should be considered as representative of the magnitude.

Algorithm Errors

In this section we discuss the errors in SO_2 retrievals within volcanic plumes using radiative transfer simulations for low-latitude (e.g., Mount Pinatubo) observing conditions (K95). Simulated albedos are passed through the TOMS SOI algorithm to evaluate the biases as a function of solar zenith angle, satellite zenith angle, surface reflectivity, lower boundary pressure, SO_2 amount, and plume altitude. The albedos are computed using three types of volcanic plume models; gas phase only, gas plus volcanic ash, and gas plus sulfate aerosol. The range of SO_2 amounts considered extends to 600 DU. Such high amounts are observed only rarely in very fresh plumes; most plumes contain less than 100 DU of SO_2.

Figure 9 shows simulated percentage SOI errors for two sulfur dioxide amounts as a function of the satellite zenith angle for different solar zenith angles. An ash- and aerosol-free SO_2 plume has been placed at 25 km altitude. Total SO_2 column amounts of 50 and 100 DU are presented in the top and bottom panels, respectively. These simulations indicate that the SOI algorithm estimates SO_2 values within ±3% for most scan angles and is stable over moderate solar zenith angles. However, a larger scan angle dependence develops at large solar zenith angles.

The results at larger amounts (up to 300 DU) are shown for nadir viewing conditions in Figure 10 where percentage error is plotted versus vertical absorber amount. The ozone and sulfur dioxide have been combined in a total absorber (effective ozone) amount in which SO_2 is weighted by 2.5 times O_3 to account for cross-section differences. Polynomial fits to the model results are shown by the solid curves. For moderate solar zenith angles the errors are within ±5% over the entire range of ozone and sulfur dioxide amounts. These small errors indicate that the quadratic correction in the SOI algorithm is effective in compensating for nonlinearities under these conditions. However, at large solar zenith angles the algorithm overestimates the true amount by up to 20% for very large SO_2 amounts, and the error becomes dependent on plume thickness.

The dependence of SOI values on the azimuthal angle has been found to be weak even for large solar zenith angles; therefore one can neglect it with confidence for small and moderate solar zenith angles.

The effects of tropospheric clouds on the SOI were evaluated by changing the surface pressure and reflectivity. The presence of a highly reflecting cloud (R = 0.8) only results in a 5% SOI decrease for the central scan positions and somewhat higher decreases at the edge of the scan. Changes of the surface pressure from 1 atm to 0.1 atm can also decrease the SOI and result in underestimation particularly at the edges of the TOMS swath.

The effect of plume altitude on SOI retrievals has been simulated by changing the height of the SO_2 layer from 2 to 30 km, keeping the total SO_2 amount and width of the vertical distribution the same (50 DU SO_2 and half-width 2 km). Figure 11 shows that the retrieval becomes more dependent on lower boundary reflectivity as the plume moves to lower altitudes. For typical conditions where R = 0.2, the small overestimate for a 25-km plume grows to a maximum overestimate for plumes at 10 km, then decreases to become an underestimate below 3 km. As the surface reflectivity increases, the

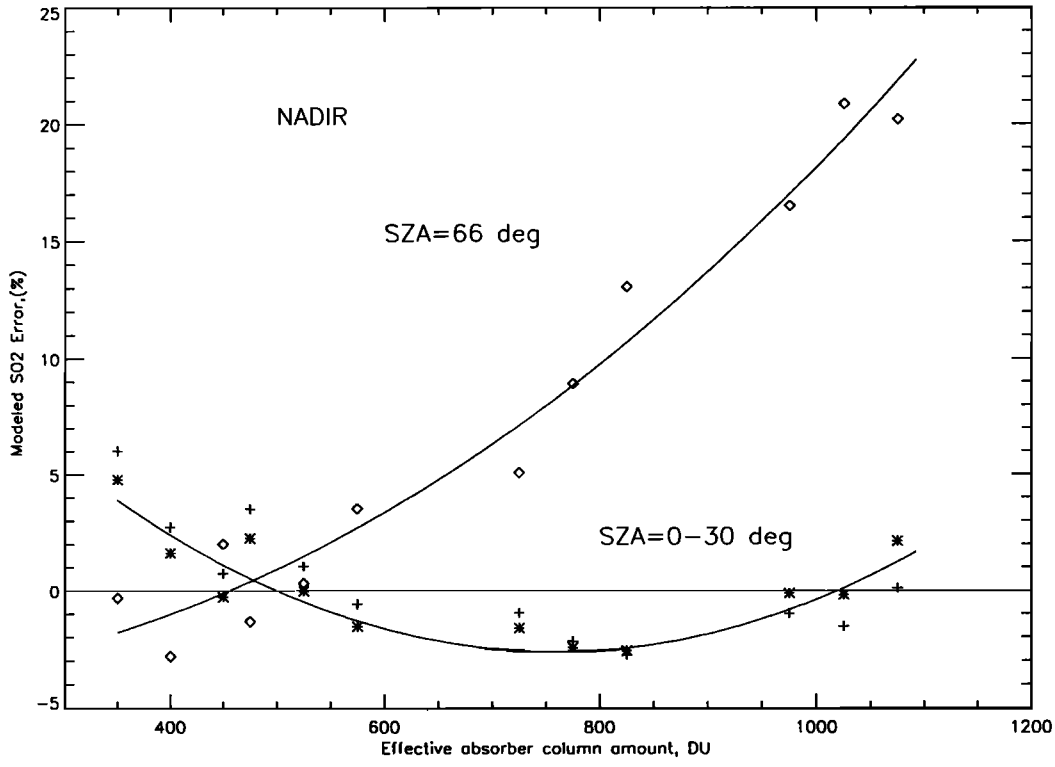

Figure 10. Simulated TOMS SO_2 error as a function of the atmospheric absorber column amount for nadir scan position and solar zenith angle equal to 0° (pluses), 30° (asterisks), and 66° (diamonds). Model results for 225-, 275-, and 325-DU low-latitude ozone profiles, clear sky conditions (1 atm surface pressure and zero surface reflectivity), no volcanic aerosol, and different SO_2 column amounts encountered in volcanic plumes (50, 100, and 300 DU). The SO_2 layer has a Gaussian vertical distribution with maximum at height 25 km and half width 2 km. The lines are least squares polynomial fits of the model results for similar solar zenith angle (SZA) conditions.

overestimates increase, and the altitude of the peak overestimate moves lower. Over ice or a low, highly reflecting cloud the SO_2 content is overestimated by a factor of 2 if the plume is near the surface. On the other hand, a low-altitude plume would be underestimated by 30–50% over clear ocean or low-reflectivity land. These complex effects are due to an increase in the path of the photons within the plume as air density increases at lower altitudes, and amplified by the additional light reflected from a more reflective surface. Thus knowledge of the plume altitude could be used to improve the SO_2 retrievals, particularly for tropospheric plumes.

Ash and Aerosol Effects on Retrieval

Volcanic sulfur dioxide plumes are generally accompanied by ash and aerosols, particularly during the early days after an eruption. In addition, sulfate aerosols produced from sulfur dioxide in the stratosphere may be present long after the eruption. Thus a gas-only radiative transfer model may not describe the true errors in the SOI retrievals. Figure 12 shows both modeled and measured zonal averaged (30°S–30°N) SOI levels in background conditions before the Mount Pinatubo eruption (on June 9) and two months after the eruption (on August 15) when most of the SO_2 had been converted to sulfate aerosols. The effect of the sulfate aerosol layer is to increase the background SOI values over the central scan angles by about 3 DU in both the model and the measurements, although a greater scan angle dependence appears in the data. The sensitivity to sulfate aerosols is about 1.5 DU per 0.1 unit change in the 550-nm aerosol optical thickness.

Ash in fresh volcanic plumes also results in an overestimate of sulfur dioxide. The percent error as a function of scan angle is shown in Figure 13 for volcanic ash and sulfate aerosols added to our low-latitude atmospheric model assuming 50 DU column SO_2. Aerosol and SO_2 are both assumed to have a Gaussian vertical distribution with a 25-km peak height and 2-km half width. Two volcanic ash particle models [*Patterson*, 1981; *Patterson and Pollard*, 1983] and the *Bhartia et al.* [1993] sulfate aerosol distribution have been considered. The aerosol optical thickness (AOT) at 550 nm of all three models is equal to 0.3. Volcanic ash increases SOI by 15 to 30% depending on the ash microphysical parameters due to spectral changes, especially at 312 nm. Similar trends can be also seen in the results of model calculations for SO_2 = 100 DU. This effect decreases for lower-altitude volcanic plumes, becoming negligible below approximately 15 km, and increases with solar zenith angle and aerosol optical depth.

The model results show that the present TOMS SOI retrieval algorithm works well for aerosol-free SO_2 plumes. Nonlinearity errors tend to overestimate SO_2 retrievals by less than 10% for typical low-latitude conditions. However, the algorithm tends to overestimate the column SO_2 content even more due to volcanic aerosols located near the altitude of the ozone maximum (about 25 km). At the same time, the observational azimuth angle, solar zenith angle (less than 40°), sur-

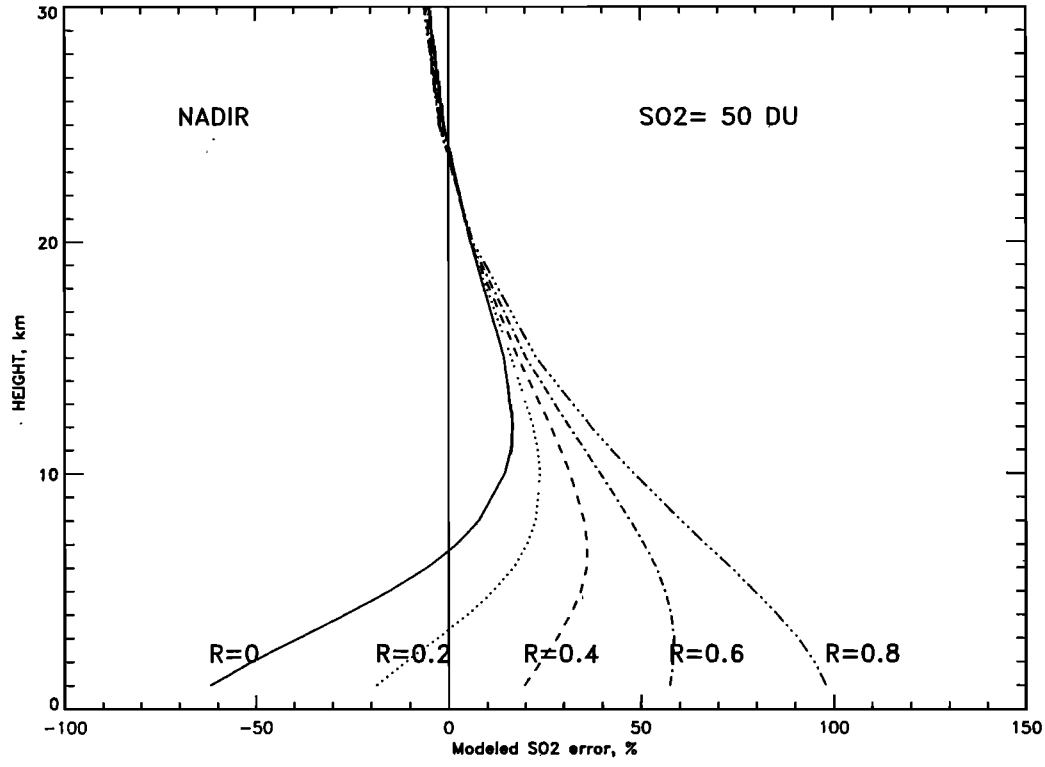

Figure 11. Simulated TOMS SO_2 error versus volcanic plume height for underlying surfaces of differing reflectivity ranging from 0 to 0.8. Model conditions are solar zenith angle equal to 16°, 275-DU low-latitude ozone distribution, 50-DU SO_2 without aerosols, in 2-km half-width Gaussian vertical layer centered at heights from 2 to 30 km; surface pressure is 1 atm.

face pressure, and surface reflectivity have a little effect on the SOI retrieval. Additional information about AOT derived either from the TOMS nonabsorbing wavelengths (360 and 380 nm) or from using supporting information is crucial for increasing the accuracy of the retrieval.

Total Ozone Errors

Although the linear SO_2 algorithm (equation (10)) does not require the input value of the true ozone column amount, its global empirical correction used to generate the SOI value

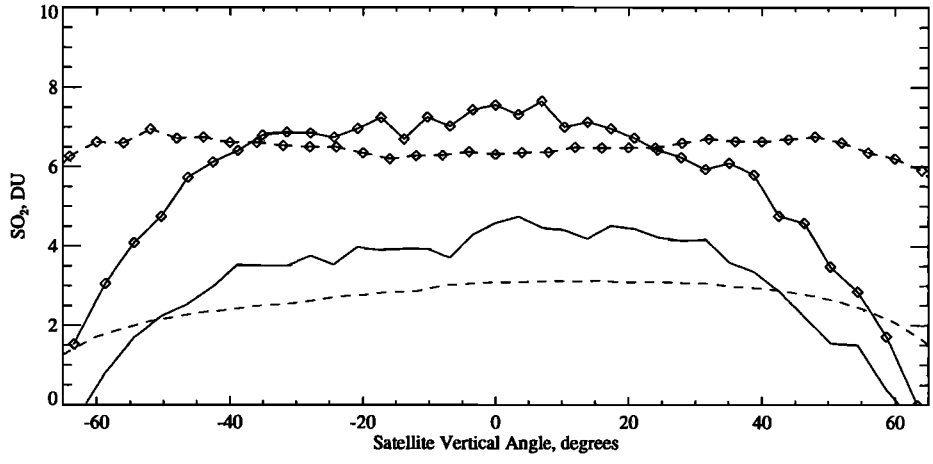

Figure 12. Comparison between measured (solid curves) and simulated (dashed) background SO_2 for pre-Pinatubo aerosol conditions (June 9, 1991) and post-Pinatubo aerosol conditions (August 15, 1991, diamonds) in the latitude band 30°S to 30°N. The TOMS data were filtered for low-reflectivity conditions (less than 30%). Model results are for solar zenith angle equal to 30°, 275-DU low-latitude ozone profile, clear sky, surface reflectivity R = 20%. Post-Pinatubo volcanic aerosol is modeled by Gaussian sulfate aerosol layer with half width 2 km at 25 km with optical thickness at 550 nm equal to 0.2.

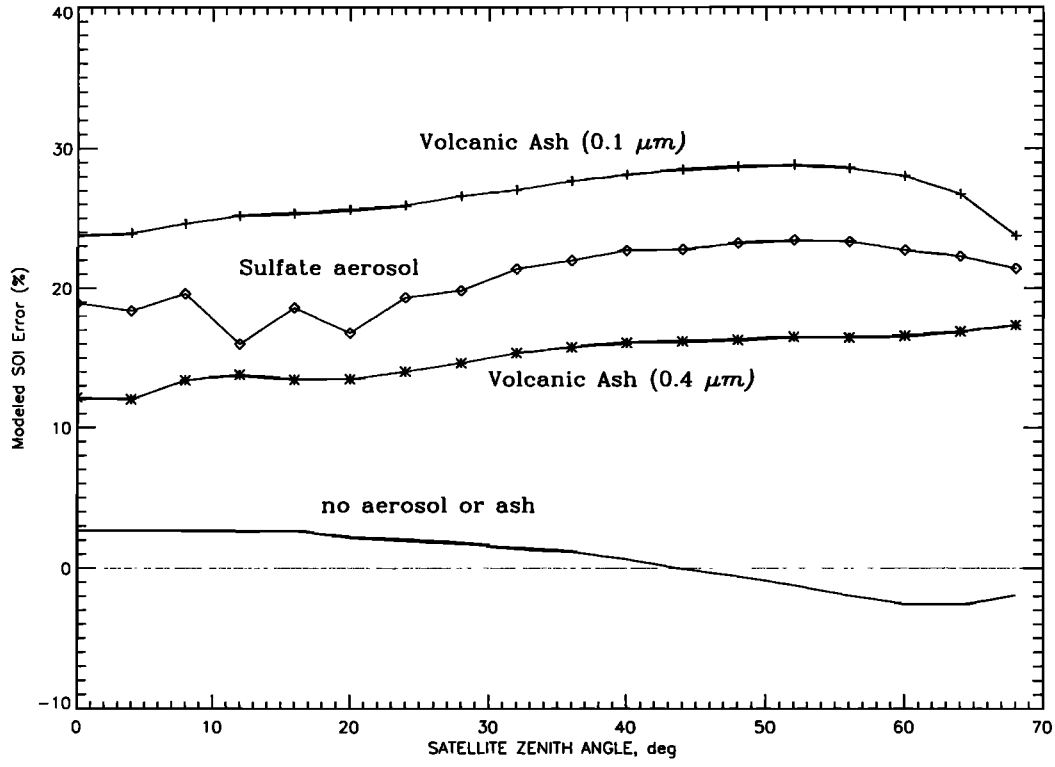

Figure 13. Simulated error in retrieved SO_2 versus satellite zenith angle for clear sky, volcanic ash, and sulfate aerosol conditions compared with aerosol-free case. Two volcanic ash aerosol models with small (effective radius about 0.1 μm) and large particles (effective radius about 0.4 μm) are presented. Model conditions: SZA = 0°, SO_2 = 50 DU, aerosol layer at 25 km with 2-km half width, aerosol optical thickness at 550 nm = 0.3 for all models.

(equation (11)) does require the value of the apparent total ozone amount to be estimated a priori. We presently use the amount computed by the total ozone algorithm, or estimate the amount when the algorithm fails to produce a result. It is useful to examine the error in SOI due to an error in the effective ozone.

The effect of ozone changes in the plume on SOI retrievals has been simulated by changing the apparent total ozone amount in (11) by 50 DU for 225, 275, and 325 low-latitude ozone profiles and different SO_2 column amounts encountered in the volcanic plumes (50, 100, and 300 DU). The gas phase only plume has a Gaussian vertical distribution with maximum at height 25 km and half width 2 km. These simulations indicate that an error in the true total ozone content of ±50 DU results in a ±5% SOI error for the central scan positions and small to moderate solar zenith angles at low latitudes.

Plume Mass Estimation

Cloud Detection

The smallest volcanic plume that can be detected in a single TOMS footprint depends on the noise level of the data, the plume altitude, and the surface reflectivity. For a typical standard deviation of 6 DU, as shown in Figure 8, a nadir pixel would need to contain 400 t SO_2 to be at the 4 standard deviation level, if it is detected with 100% efficiency. Such a pixel would not be considered uniquely sulfur dioxide unless near a volcano that had been reported to have erupted. In addition, such a small plume is almost certainly near the ground, over low-reflectivity terrain. Figure 11 indicates that the SO_2 amount would be underestimated by an amount which depends on reflectivity. However, SOI values greater than 4σ are assumed to be signal rather than noise if they are contiguously clustered in the vicinity of an active volcano. If we assume a background SOI sigma of 6 DU, then a cluster of four pixels with 24 DU greater than average represents 2400 t of SO_2. This is the approximate detection limit of volcanic SO_2 plumes for the TOMS SOI data.

Cloud Mass Calculation

Two methods have been used to compute SO_2 plume masses from the TOMS data. The method used within TOMS SO_2 papers published through 1993 require the TOMS SO_2 column amounts to be gridded onto a 1° × 1° rectangular array. The contribution to each grid box in the array from the neighboring TOMS points is calculated using a distance weighting. A second technique relies on knowledge of the area of the footprint of each TOMS scan position across the swath (see Figure 2). In both cases, cloud masses, in metric tons, are calculated by multiplying the column SO_2 amount determined for each grid box or footprint by its area and then summing within the plume area, as shown in (15):

$$M\ SO_2\ (\text{tons}) = 0.0285 \sum \text{SOI}_i\ (\text{DU})^* A_i\ (\text{km}^2) \qquad (15)$$

For the overlapping footprints the area of overlap is considered to be part of the footprint closest to the center of the scan. The total plume tonnage is the sum of the SO_2 mass for all footprints with centers within the designated plume box.

One difficulty with both methods is overlapping orbits, which

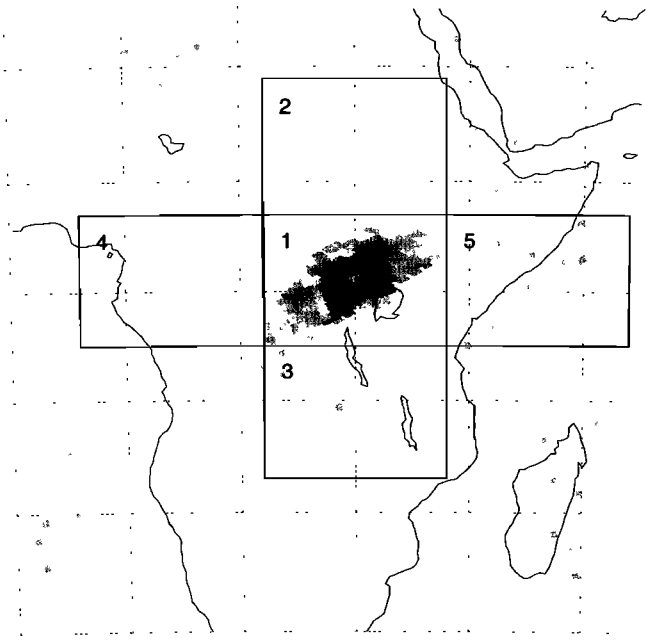

Figure 14. Sulfur dioxide plume from Nyamuragira volcano on December 27, 1992. The location of the volcano is at 1.4°S, 29.2°E. Note that boxes 1–5 are used for the SO_2 plume mass calculation process.

occur at high latitudes. For Nimbus there is a lapsed time of 104 min between orbits, and during this time it is possible that a volcanic plume could have moved, been vertically sheared, or chemically converted. Hence interpretation of the data can be unclear. To avoid these problems, TOMS data at high latitudes are analyzed on an orbit-by-orbit basis. This is not a significant problem at low latitudes where there is little interorbit overlap.

In both methods, regions adjacent to the plume are also measured in order to calculate a background mass of SO_2 due to the various biases. This background SO_2 tonnage per square kilometer, usually the average amount calculated from several background boxes, is then subtracted from the tonnage determined from the plume box. We make the assumption that the neighboring background boxes are sufficiently similar in terms of solar zenith angle and cloudiness to the plume box such that the calculated average background SO_2 amount will be valid inside the plume box itself. This implicitly assumes that the conditions inside the plume box are not greatly perturbed by the presence of the volcanic plume.

As an example, consider the December 27, 1981, SO_2 plume from the Nyamuragira volcano in Zaire shown in Figure 14. Box 1 is the designated plume box and boxes 2–5 are used to calculate the SO_2 background level. Using the footprint method described above, the mass per unit area of each box is calculated and these are shown in Table 4. To remove some of the geophysical variation in the background SO_2 level, empirical corrections discussed earlier are used. Results are shown with no corrections applied and with reflectivity and scan bias corrections applied.

Without corrections the background results from these boxes vary widely, from -0.185 to 0.01 t km^{-2}. This gives a background range of -463 to 25 kt, with an average of -151 kt. The total plume tonnage is $0.340 \times 2.5 \times 10^6 = 850$ kt $-(-151$ kt), giving ~1000 kt. When the empirical corrections are applied, the magnitude of the background box mass increases in all boxes. The large negative mass in box 3 is due to high reflectivity, which even after correction still gives a negative bias. The effect of applying the corrections is to increase the plume mass by over 300 kt. Using both corrections changes the size of the background SO_2 mass to -10 kt, thus significantly decreasing the effect of the background correction upon the plume tonnage.

As the TOMS instrument is a mapper and not a sampler, to a first order the errors in measuring the complete plume are a compilation of the errors which go into a column measurement. However, there are other difficulties not discussed in the sections dealing with column SO_2 measurements which can cause additional errors. These are related to the size of the instrument noise.

TOMS background SO_2 values have a standard deviation in the range of 5 to 7 DU. Within a zonal band 10° wide, there will be ~10,000 points and thus the standard error of the mean SO_2 is very small, ~0.05 DU. However, the SO_2 average we calculate for tonnage calculations is not the zonal mean but a local mean for the neighboring background boxes with similar geophysical parameters (e.g., ozone, solar zenith angle) to the plume box. The standard error of the box averages is expected to be about 0.15 DU, given 450 samples in each of the four boxes. The standard error of the mean of the corrected background averages in the above example (0.9 DU) is larger than expected, primarily due to additional noise introduced by geophysical effects such as clouds. This 0.9-DU uncertainty in background translates to 60 kt SO_2, which is less than 5% of the calculated plume mass. However, this same background uncertainly could be a significant percentage of the plume mass in a smaller eruption.

As the size of a volcanic plume increases, it becomes harder to calculate the background SO_2 level. First, as the plume box increases in size, the geophysical parameters within the box are more likely to vary and thus our assumption that the mean background is constant becomes increasingly important. Second, a larger plume takes up more of the Earth's surface and neighboring background boxes may be moved to entirely different regions (higher/lower latitudes, cloudy/cloud-free scenes). Thus the neighboring boxes may no longer be an accurate representation of the plume box itself. When a plume grows so large as to fill a zonal band (El Chichon or Pinatubo), it is not possible to use a number of neighboring boxes and it is necessary to use zonal means to correct for background. As the spatial dimensions of the volcanic plume increase (due mainly to vertical wind shear), the error introduced by the background uncertainty increases.

Another error related to the discussion above concerns those TOMS footprints which contain some SO_2, but in concentration below the noise level, and thus are assumed to have zero SO_2. These points are usually around the perimeter of the

Table 4. Results of Cloud Mass Calculations for December 27, 1981

	SO_2 Mass Per Unit Area, t km^{-2}					Cloud Mass,
Correction	Box 1	Box 2	Box 3	Box 4	Box 5	kt
None	0.340	−0.032	−0.185	−0.036	0.010	1000
Both	0.529	0.018	−0.076	0.002	0.039	1332

Note that area of box 1 is 2.5×10^6 km^2.

observed plume, and because we do not recognize these points as part of the plume, they tend to fall into background boxes. This causes an artificially high background level and an underestimation of the true plume mass. One way to minimize this effect is to enlarge the "plume" box and to select the "background" boxes from areas far removed from the plume. However, then the background boxes no longer have the same geophysical parameters as the plume box, leading to unrepresentative background values. In young plumes of significant masses the percentage of SO_2 lost by assuming zero SO_2 in these perimeter points is relatively small, of the order of a percent or less. However, as the plume thins to where most of the observed points are just above the noise level, the error caused by these nonzero SO_2 but unrecognized plume pixels becomes quite large; conceivably, the amount of missed SO_2 can be much more than the amount observed.

It should be reemphasized that the size of the potential error of a plume mass calculation changes with variations in a number of parameters, as discussed in previous sections of this paper. For example, if a plume is near the extreme edges of the scan, the potential uncertainty is much larger than if it was in the center of the scan. Figure 3 shows that at the near-nadir scan positions, where TOMS sensitivity to SO_2 mass is the highest, a measurement change of 1 DU is actuated by a little more than 50 t SO_2. However, at the extreme view angles it takes almost an order of magnitude more SO_2 in a footprint to cause a measurement change of 1 DU. Thus if a heterogeneous plume is spread across the complete scan, it is very difficult to estimate error. The error is much easier to estimate if the plume is contained in the center of the scan. If the plume boundary is diffuse (as is typical for an "old" or "effusive" plume), then defining the extent of the plume can be difficult and subjective. In short, errors associated with each plume measurement must be evaluated individually and it is impossible to give a general figure for TOMS plume measurement error.

Volcanic Eruption Mass Estimation

Our primary interest is not the amount of SO_2 in volcanic plumes as observed at the times of overpass but on the total amount of sulfur that is erupted into the atmosphere. It is in this final step where potentially the greatest errors lie. As the satellite observes the plume nominally only every 24 hours, some assumptions must be made in order to calculate the SO_2 amount erupted. The degree of uncertainty, and the subsequent error in the measurement, depends on several circumstances: the first being the type of eruption which is occurring; that is, an explosive eruption where a very high percent of the gas ejection takes place in a short period of time (generally minutes to hours) or an effusive eruption where gaseous and lava production can occur fairly continuously for days, weeks or even months. Volcanoes on subduction settings (e.g., Mount Pinatubo, El Chichon, Mount St. Helens) are usually of the explosive type; more basaltic volcanoes on hot spot or rift environments (e.g., Mauna Loa, Nyamuragira, Krafla) are typical of the effusive type.

Explosive Eruptions

Analysis of the explosive, subduction type is simpler, at least in concept. When estimating the amount of SO_2 emitted by an explosive eruption, the original plume of gas is assumed to be a point source injection at a particular time and it is only necessary to calculate or estimate the amount of SO_2 lost between the time of ejection and the time of observation(s). This calculation assumes that measured (observed) tonnages are minimum values because between the time of ejection and the observation both chemical conversion of SO_2 to H_2SO_4, with subsequent rainout, and physical dissipation of SO_2 at the plume margins to below the TOMS detection limits have taken place.

That part of the loss rate due to conversion of SO_2 to H_2SO_4 is highly dependent on plume altitude. If the erupted SO_2 remains below the tropopause, there is more rapid oxidation and chemical conversion to sulfuric acid, with subsequent rainout, than in the drier, relatively less reactive conditions in the stratosphere. The loss rate is also dependent on the geometry and mass of the plume. Plumes that encounter regions of wind shear can become extended, so that the plumes have a high perimeter to mass ratio, and quickly dissipate to a concentration below the TOMS detection limit. Large stratospheric plumes, where conversion from SO_2 to H_2SO_4 is slow and the amount lost at plume boundaries due to dissipation is small compared to the total mass of the SO_2 plume, tend to be long lived (e.g., the SO_2 plume emitted from Mount Pinatubo in 1991 decreased by less than 10% a day during the first week of observation [*Bluth et al.*, 1992]). In contrast, tonnages of small, tropospheric sulfur dioxide plumes with a high perimeter to mass ratio are more affected by physical and chemical processes and commonly decrease by up to 50% per day [e.g., *Bluth et al.*, 1994].

If a plume from an explosive eruption is observed for several days, the amount erupted is calculated by fitting an exponential curve to the measured plume masses [*McKeen et al.*, 1984] and the curve is extrapolated back to the time of eruption. If the plume is only observed on a single day because of rapid dissipation or conversion, then this amount can be considered only a minimum value and the amount produced is estimated on the basis of a loss rate of 50% per day for tropospheric clouds. This is the approximate average rate observed for several low-altitude eruptions of sufficient mass so that they could be followed for several days.

The uncertainty involved in estimating the original emission of SO_2 generally decreases with the number of available observations; thus the more days an SO_2 plume is detectable by TOMS, the better the extrapolation. Given repeat measurements with error estimates on those measurements, the error involved in the extrapolation back to the time of the explosive eruption can be calculated with some confidence. An analysis of the Pinatubo extrapolation is shown in Figure 15. Cloud tonnages were determined on 5 days during the first 14 days after the eruption. An exponential fit to these data points produces an estimate of the initial value of 17.6 Mt with the scatter in the data points around the fit producing a 95% confidence interval in the initial value of $\pm 15\%$. If only the four points taken in the first 7 days are used, the initial mass estimation rises to 18.8 Mt, but the 95% confidence interval is now $\pm 33\%$.

There is another consideration in estimating the total emission of SO_2 in both the explosive and the effusive types of eruptions. Some of the sulfur emitted by certain volcanoes may be in the form of H_2S, which is not detected by TOMS, rather than SO_2 [*Luhr*, 1991; *Doukas and Gerlach*, 1995]. Hydrogen sulfide is oxidized to produce SO_2, thus adding to the plume total that is measured with TOMS with time. A possible example is found in the eruptions of Mount Spurr [*Bluth et al.*, 1995].

In addition, any sulfur dioxide that is converted to sulfate

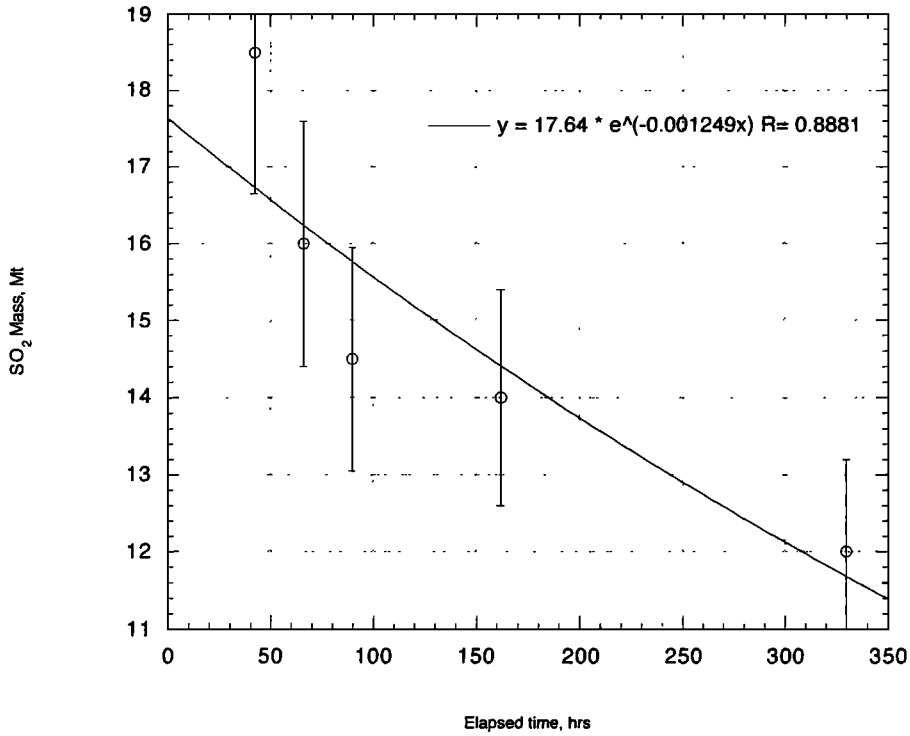

Figure 15. Estimation of initial Pinatubo SO_2 mass by extrapolation of exponential fit of observed plume masses versus time after eruption. Error bars are estimated 10% standard deviations in plume mass.

within the eruption column will not be detected. Thus the TOMS measurement is very likely a lower estimate of the total SO_2 in the eruption.

Effusive Eruptions

The total amount of SO_2 produced by an effusive, long-lived eruption is much more difficult to estimate than the explosive eruptions just described. In an effusive eruption the change in mass between observations is not only due to loss of the gas from conversion and dissipation but also due to gain from new production at the volcano. Now it is necessary to somehow separate the mass of the "new" SO_2 (produced since the last observation) from the "old" dissipating SO_2 plume measured in the last overpass. Often the unraveling of the two is aided by the spatial distribution of the plume mass. Figure 16 is from the effusive eruption of Nyamuragira of December 1981 to January 1982, from which we observed new SO_2 plumes over a 13-day period. It shows part of the SO_2 plume as seen on December 30, five days after the start of the eruption. A thin plume is observed over about 1.3 million km^2 of central Africa, mainly to the west and north of the volcano. Superimposed on this thin plume is a much denser cloud coming directly from the volcano and stretched out to the northwest. This denser cloud covers only about 60,000 km^2. A reasonable assumption is that the large thin cloud and even thinner and more discontinuous clouds to the east over the Indian Ocean and to the west over the Atlantic Ocean are old SO_2 from the previous four days of eruption, while the new material since the last observation is the denser plume. However, where the line is drawn between dense and thin clouds is subjective. Clearly placing a box around such a diffuse plume is not a straightforward exercise. Care must also be taken to ensure that the neighboring boxes used to calculate a background level are actually SO_2 free.

A parametric method can be used to estimate residual amounts of SO_2 as a function of chemical conversion rate (A. J. Krueger et al., The December 1981 eruption of Nyamuragira Volcano (Zaire) and the origin of the "mystery cloud" of early 1982, submitted to *Journal of Geophysical Research*, 1995). An initial estimate of the SO_2 production over the past 24 hours is made based on plume morphology. Then using this new production figure, the total amount in the scene, and the total amount in the previous scene, we derive the conversion/dissipation rate, and if this gives an unreasonable rate considering the estimated altitude of the plume, we reevaluate the data on new production, based on reasonable dissipation rate and continue this process until both production and dissipation rates are reasonable in terms of the data and our prior experience. In the above case of Nyamuragira the total amount of SO_2 observed on December 30 is about 1.5 Mt, while our estimate of the amount produced in the past 24 hours is only a little over 200 Kt, based on our judgment of where to separate new from old and on the loss rate over the 24 hours.

Error estimates for effusive eruptions are, by necessity, very complicated and subjective as there are a number of parameters to consider (e.g., plume measurement errors, dissipation rate per day, and temporal changes in production). The parametric method described above provides a measure of the sensitivity of production rate to dissipation rate and therefore of potential error involved in our final estimate of amount produced.

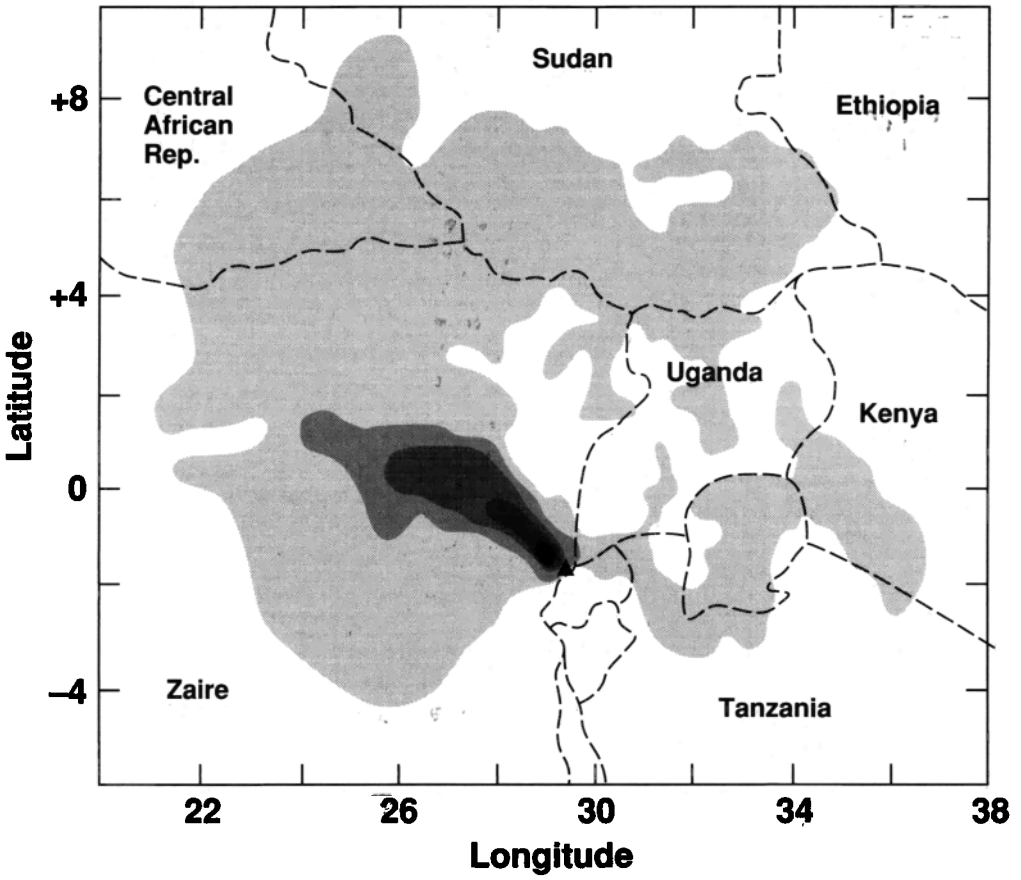

Figure 16. Sketch map of central Africa showing the volcanic SO_2 plume from Nyamuragira (Zaire) volcano on December 30, 1981. Concentrations in DU, with a contour interval of 30 DU. The location of the volcano, essentially on the border of Zaire and Rwanda, is shown by the triangle.

Comparisons of TOMS Data With Other SO_2 Measurements

Volcanic plumes are transient features which only rarely drift over ground-observing stations. Yet the scale of explosive eruptions overwhelms efforts to measure their size from fixed or mobile sites near the volcano. Thus the problem of validation of satellite techniques is severe. Some approaches and resulting comparative data are discussed in this section.

COSPEC Observations

Attempts to compare TOMS SO_2 retrievals with those of the portable correlation spectrometer (COSPEC), routinely used by volcanologists to measure effusive volcanic plumes, have not met with success due primarily to the vastly different sensitivities. A period of explosive volcanism at Galunggung volcano, Indonesia, from August 19 to September 19, 1982, has thus far provided the best opportunity to compare TOMS and COSPEC measurements [*Bluth et al.*, 1994]. During this time, 10 large eruptions were reported, with estimated VEIs ranging from 2 to 4. Nine of these eruptions produced SO_2 plumes that were also observed by TOMS, emitting a total of 120 kt SO_2. The COSPEC was operated for 25 measurement periods over 23 days during this interval, with measurement periods ranging from 5 to 165 min in length. However, the COSPEC was never employed during an actual explosive eruption; the instrument was in operation either several hours before or after the large events. After extrapolation to estimate daily amounts, the SO_2 emissions from COSPEC totaled only 20 kt [*Badruddin*, 1986]. *Bluth et al.* [1994] used the results from the two instruments to compare explosive and nonexplosive degassing from Galunggung, but it was not possible to directly compare measurements of the same plume by the two instruments as the COSPEC was not in operation during the explosive phases which were observable by TOMS.

Brewer Spectrophotometer Observations

Sulfur dioxide column amounts are measured routinely with Brewer spectrophotometers at a number of stations around the world. Validation of TOMS with Brewer instruments depends on the transient volcanic sulfur dioxide plumes drifting over a station at the same time that TOMS is passing overhead. In the 14 years of TOMS data, only one case has been found where such simultaneous measurements have occurred although volcanic plumes have been observed from Brewer stations and TOMS on the same day in two other cases. The plume from an eruption of Mount Spurr in Alaska on September 17, 1992, passed over Toronto on September 19 where Brewer observations are made continuously each day. Nimbus 7 flew over this station in the morning and Meteor 3 arrived about five hours later in the afternoon. At Toronto's latitude, two sightings were made from each satellite. The results are shown in Figure 17 where the Brewer data show the arrival and passage of the plume over the station (J. B. Kerr, private communication, 1992). The Nimbus TOMS results are the two data points at

1400 and 1540 UT; Meteor arrived after the plume had passed but are shown as the data points at 1900 and 2100 UT. A 10-DU bias between the Meteor and the Nimbus background levels due to calibration differences has been removed. The satellite data are within 20% of the Brewer data, indicating that the TOMS algorithm is reasonably accurate, at least for low and moderate sulfur dioxide amounts.

The two cases where Brewer stations and TOMS observed the same plume on the same day but not simultaneously were from the St. Helens eruption of May 18, 1980, and the Krafla eruption of September 5, 1984 [*Kerr and Evans*, 1987]. The leading edge of the plume from the St. Helens was about 300 km southwest of the Brewer station at Toronto as TOMS passed overhead on May 20, so that only background data could be compared. However, typical TOMS values in the plume were 60 to 70 DU and the readings at Toronto peaked at 70 DU six hours later. *Kerr and Evans* [1987] stated "the results were in good agreement with regard to both the measured time of arrival of the plume in the Toronto area as well as the measured values of SO_2 within the cloud." Likewise, the Krafla plume measurements agreed at the 40-DU level.

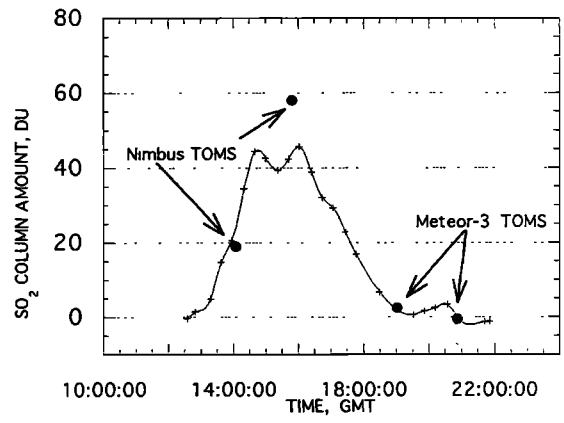

Figure 17. Comparison of Nimbus 7 and Meteor 3 TOMS sulfur dioxide measurements (circles) with ground-based Brewer spectrophotometer measurements (pluses) of the September 17, 1992, Mount Spurr eruption plume as it passed over Toronto on September 19.

SBUV Observations

SBUV instruments routinely collect data at the same wavelengths used by TOMS for SO_2 observations. However, image motion during the serial sampling of the wavelengths produces large errors in SO_2 retrievals. About once a month, data are collected in a continuous spectral-scan mode, so that the strong spectral bands of SO_2 between 300 and 310 nm (see Figure 1) are observed in the Earth albedo over volcanic clouds. Sampling is sparse, limited to the ground track of the satellite and then only about every 12° of latitude along track. Therefore with these limitations, SBUV has observed only two eruptions, El Chichon [*McPeters et al.*, 1984] and Pinatubo [*McPeters*, 1993]. SBUV data from a total of 5 days of volcanic plume observations have been reported for these two eruptions. Comparison is complicated because SBUV and TOMS have quite different footprints and, in the case of Pinatubo, flew on different satellites which passed over the plume some hours apart.

SBUV data from Pinatubo are less useful than from El Chichon, primarily because the SBUV captured fewer points from Pinatubo with SO_2 column amounts above the TOMS background level. Most of the Pinatubo SBUV data were from the fringes of the plumes where the sensitivity of the TOMS was insufficient to reliably measure SO_2. Also, as the El Chichon data were taken when both sensors were on the same satellite and SBUV was "boresighted" with the TOMS, the TOMS data which are averaged to match the SBUV data come from the center of the scan, where ozone pathlength corrections and Sun angle variations are minimized. In contrast, the TOMS data for the Pinatubo plume were taken at various positions in the scan, some at extreme angles where TOMS errors are maximum. Finally, when comparing data from the Pinatubo eruption, it is necessary to account for the movement of the plume during the several hours difference in time of overpass of the two satellites. Out of the five days where both sensors measured SO_2 in the same plume, only one day's data, from the April 15, 1982, of El Chichon, had a sufficient spread in SO_2 concentrations to allow any significant measure of correlation.

Figure 18 is a comparison of the SBUV values with the averages of TOMS values from the same 200 × 200 km footprints of SBUV for the April 15 overpass of the El Chichon plume, 11 days after the April 4 eruption. Sixteen TOMS pixels were averaged to comprise an area equal to the SBUV footprint. There is a good correlation ($r = 0.92$). The background (zero) levels of the two sensors agree within approximately 1 DU. However, the least squares line has a slope almost half that expected, with TOMS values higher than SBUV by a factor of about 1.8.

Thus this comparison shows only a first-order agreement between TOMS and SBUV. The background levels agree within 1 DU, but at levels above background the TOMS data are considerably higher than measurements obtained from the SBUV sensor. This may be due simply to a paucity of data above TOMS noise level (approximately 5 DU). Only 5 of the 17 points had TOMS-measured SO_2 column amounts greater than twice the noise level. Also, errors in the SBUV are unknown. Thus this comparison is suggestive that the two instruments do not give the same values, but the test is not conclusive. It is unfortunate that in the two largest eruptions of the last several decades we did not have a coincidence of data over an area rich in SO_2, in the range of 50 to 100 DU, so that an unambiguous comparison could be made.

Eruption Mass Comparisons

During the period of TOMS operation the eruptions of El Chichon and Mount Pinatubo have afforded the best opportunities to compare TOMS estimates of erupted SO_2 masses with those of other instruments. Four satellite sensors made measurements of one or both of these eruptions which can be compared to TOMS: the Stratospheric Aerosol and Gas Experiment II (SAGE II), the advanced very high resolution radiometer (AVHRR), the microwave limb sounder (MLS) on board the UARS, and the solar backscattered ultraviolet spectrometer (SBUV).

SAGE II can measure the mass of stratospheric sulfuric acid aerosol derived from the SO_2 from large volcanic eruptions. *McCormick et al.* [1984] used lidar measurements after the El Chichon eruption in 1982, and *McCormick and Veiga* [1992] used SAGE measurements taken over 2 months after the eruption of Pinatubo to estimate the amount of sulfuric acid aerosols produced by these eruptions. However, the amount of aerosol derived from SAGE must be less than the amount of

erupted sulfur dioxide, as losses occur between eruption and detection as aerosol by SAGE. *Stowe et al.* [1992] derived aerosol optical thickness maps from AVHRR data and followed the formation and loss of the Pinatubo sulfate aerosols with high spatial resolution.

The MLS began operation several months after the eruption of Pinatubo and collected data on SO_2 concentrations in the stratosphere. *Read et al.* [1993] reported MLS-measured SO_2 amounts observed 3–6 months after the eruption, and their extrapolation of the MLS data back to the time of eruption generally agreed with that of the TOMS. *McPeters* [1993] used 2 days of SBUV sampling of the Pinatubo plume, 16 and 32 days after the eruption, and extrapolated back to the time of the eruption.

As can be seen in Table 5, all four satellite methods agree, within instrument error, on the total SO_2 emissions from the largest two eruptions during the satellite age. This agreement is somewhat remarkable given each instrument's limitations and resolutions, the dynamic nature of the El Chichon and Pinatubo eruption plumes, and the fact that each volcanic data set is essentially a by-product from the original mission objectives.

Future Work

Although the SOI algorithm performs well under most low-latitude conditions, its degradation at high latitudes must be evaluated where approximately 30% of the eruptions occur (*Smithsonian*, 1989). In addition, the Nimbus TOMS data wavelengths have recently been found to be in error by about 0.15 nm. Also, the sulfur dioxide cross-section data used in the current data production have been superseded by newer measurements which include temperature coefficients. The effects of these wavelength shifts (which are larger than the perturbations assumed in the present analysis) and cross-section changes on sulfur dioxide retrievals are yet to be determined.

Algorithm Improvements

The simple algorithm for the detection of sulfur dioxide described in this paper has served its purpose extremely well by detecting large numbers of volcanic eruptions from space and by providing the first-ever quantitative estimates of volcanic SO_2. However, the error analysis presented in this paper indicates that there is potential for improvement by incorporating information from other satellite data and by algorithm changes. At large solar zenith angles the background correction noise dominates the instrument noise, thus limiting the SO_2 detection ability. Since the background correction is purely an artifact of the assumption that TOMS N value is a linear function of τ_a, from (6), it can be removed by better modeling the functional form of N versus τ.

A better modeling of the background correction, by itself, does not reduce the large sensitivity of the algorithm to SO_2 cross-section errors or to stratospheric aerosol effects. To reduce these errors, a new algorithm is being considered which discards the 312.5-nm TOMS wavelength. Although this change increases the SO_2 detection noise by about 20% at small solar zenith angles, it has the potential of better absolute accuracy (K95).

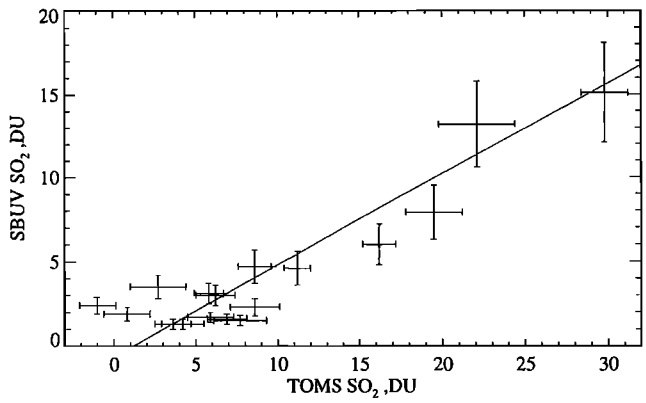

Figure 18. Comparison of TOMS and solar backscatter ultraviolet (SBUV) measured SO_2 concentrations (in Dobson units) from the same areas of the El Chichon eruption plume on April 15, 1982. Error bars are the standard deviation of the mean of the 16 values used to calculate the TOMS mean within the SBUV field of view and the assumed ±20% uncertainty in SBUV values.

Table 5. Eruption Mass Estimates (in Mt of SO_2)

Eruption	TOMS	Lidar	SAGE II	AVHRR	MLS	SBUV
El Chichon, 1982	5–9	6	N/A	N/A	N/A	N/A
Pinatubo, 1991	14–26	N/A	10–15	13.6	17	12–15

Sulfur dioxide mass; in cases of lidar, Stratospheric Aerosol and Gas Experiment (SAGE), and advanced very high resolution radiometer (AVHRR) measurements, converted from tons of H_2SO_4/H_2O solution. Ranges or uncertainties are from the original published estimates.

Summary

Volcanic eruptions vary in mass of solids erupted by at least 8 orders of magnitude. In general, eruption sizes have been estimated to 1 order of magnitude accuracy because of the difficulty of observing events of such extreme size. TOMS quantitatively maps the mass density of sulfur dioxide throughout the entire volcanic plume and repeats it each day until the sulfur dioxide falls below the detection limit. In this study the algorithm in current usage has been analyzed by radiative transfer simulations and by propagation of errors. Similar simulations have been highly successful in predicting the albedo of the atmosphere containing ozone. We have shown that the simulations reproduce the observed background SO_2 and SOI levels quite well for clear sky with and without aerosols. However, the scan angle dependence in TOMS data is somewhat larger than in the simulations. Also, clouds have a larger effect on the data than in the simulations and unexplained variations in the average background level are found. The reason for these discrepancies may be that the true TOMS instrument wavelengths are different from those assumed in the simulations and the current data production algorithm. The wavelength errors have only recently been found and the influence on the SOI retrievals has yet to be evaluated.

The model results indicate that the retrieval errors are small over a large range of volcanic conditions. In general, for low-latitude eruptions the errors depend on plume altitude and the amount of ash and aerosol in the plumes. Best case biases are about 5% but increase to 20–30% in stratospheric plumes containing large amounts of ash.

The total plume mass is determined by summing over all of the pixels in the plume and subtracting background biases which are measured in adjacent areas. The background retrievals are subject to small, apparently random biases. However, these biases can become significant when applied to large plume areas or thin plumes.

The initial mass of explosive eruptions is estimated using an exponential decay model. The statistical uncertainty is 15 to 30%, depending on the number of days the plume was measured. However, the mass emitted in long-lasting effusive eruptions is less certain because of the lack of information about decay rates.

Acknowledgments. We are grateful to the many individuals who have contributed to the analysis of TOMS sulfur dioxide data. In particular, we would like to thank James Kerr of the Atmospheric Environment Service, Downsview, Ontario, for suggesting the linear algorithm for satellite data analysis and for providing coincident Brewer spectrophotometer data; Scott Doiron, for his development of many of the volcanic cloud analysis techniques in current use; the GSFC Ozone Processing Team for providing the TOMS data sets; and Robert Fraser, Climate and Radiation Branch, GSFC, for helpful comments on the manuscript.

References

Badruddin, M., Pancaran gas SO_2 pada Letusan G. Galunggung, in *Letusan Galunggung 1982–1983*, edited by J. A. Katili, A. Sudradjat, and K. Kumumadinata, pp. 285–301, Dir. Vulkan., Dir. Jenderal Geol. Dan Sumberdaya Miner., Dep. Pertambangan Dan Energi, Bandung, Indonesia, 1986.

Bass, A. M., and R. J. Paur, The ultraviolet cross sections of ozone, II, Results and temperature dependence, in *Atmospheric Ozone*, edited by C. S. Zerefos and A. Ghazi, pp. 611–617, D. Reidel, Norwell, Mass., 1984.

Bhartia, P. K., J. Herman, and R. D. McPeters, Effect of Mount Pinatubo aerosols on total ozone measurements from backscatter ultraviolet (BUV) experiments, *J. Geophys. Res.*, *98*, 18,547–18,554, 1993.

Bluth, G. J. S., S. D. Doiron, C. C. Schnetzler, A. J. Krueger, and L. S. Walter, Global tracking of the SO_2 clouds from the June, 1991 Mount Pinatubo eruptions, *Geophys. Res. Lett.*, *19*, 151–154, 1992.

Bluth, G. J. S., C. C. Schnetzler, A. J. Krueger, and L. S. Walter, New constraints on sulfur dioxide emissions from global volcanism, *Nature*, *366*, 327–329, 1993.

Bluth, G. J. S., T. J. Casadevall, C. C. Schnetzler, S. D. Doiron, L. S. Walter, A. J. Krueger, and M. Badruddin, Evaluation of sulfur dioxide emissions from explosive volcanism: The 1982–1983 eruptions of Galunggung, Java, Indonesia, *J. Volcanol. Geotherm.* Res., *63*, 243–256, 1994.

Bluth, G. J. S., C. J. Scott, I. E. Sprod, C. C. Schnetzler, A. J. Krueger, and L. S. Walter, *Explosive SO_2 Emissions From the 1992 Eruptions of Mount Spurr, Alaska*, edited by T. Keith, *U.S. Geol. Surv. Bull.*, in press, 1995.

Dave, J. V., Development of Programs for computing characteristics of ultraviolet radiation, technical report, Vector Case, Int. Bus. Mach. Corp., Fed. Syst. Div., Gaithersburg, Md., 1972.

Dave, J. V., and C. L. Mateer, A preliminary study on the possibility of estimating total atmospheric ozone from satellite measurements, *J. Atmos. Sci.*, *24*, 414–427, 1967.

Doukas, M. P., and T. M. Gerlach, Sulfur dioxide scrubbing during the 1992 eruption of Crater Peak, Spurr Volcano, Alaska, in *The 1992 Eruptions of Spurr Volcano, Alaska*, edited by T. E. C. Keith, U.S. Geol. Surv. Bull., in press, 1995.

Georgii, H. W., Large scale spatial and temporal distribution of sulfur compounds, *Atmos. Environ.*, *12*, 681–690, 1978.

Heath, D. F., A. J. Krueger, H. A. Roeder, and B. D. Henderson, The solar backscatter ultraviolet and total ozone mapping spectrometer (SBUV/TOMS) for Nimbus G, *Opt. Eng.*, *14*, 323–331, 1975.

Kerr, J. B., and W. J. Evans, Comparison of ground based and TOMS measurements of SO_2 from volcanic emissions, in *Scientific and Operational Requirements for TOMS Data*, *NASA Conf. Publ. 2497*, pp. 60–69, 1987.

Kerr, J. B., C. T. EcElroy, and R. A. Olafson, Measurements of ozone with the Brewer ozone spectrophotometer, *Proc. Int. Ozone Symp.*, *1*, 74–79, 1980.

Krueger, A. J., Sighting of El Chichon sulfur dioxide clouds with the Nimbus 7 Total Ozone Mapping Spectrometer, *Science*, *220*, 1377–1378, 1983.

Krueger, A. J., L. S. Walter, C. C. Schnetzler, and S. D. Doiron, TOMS measurement of the sulfur dioxide emitted during the 1985 Nevado del Ruiz eruptions, *J. Volcanol. Geotherm. Res.*, *41*, 7–15, 1990.

Luhr, J. F., Experimental phase relations of water- and sulfur-saturated arc magmas and the 1982 eruptions of El Chichon volcano, *J. Petrol.*, *31*, 1071–1114, 1991.

McCormick, M. P., and R. E. Veiga, SAGE II measurements of early Pinatubo aerosols, *Geophys. Res. Lett.*, *19*, 155–158, 1992.

McCormick, M. P., T. J. Swissler, W. H. Fuller, W. H. Hunt, and M. T. Osborn, Airborne and ground-based lidar measurements of the El Chichon stratospheric aerosol from 90°N to 56°S *Geofis. Int.*, *23*, 187–221, 1984.

McGee, T. J., and J. Burris Jr., SO_2 absorption cross sections in the near UV, *J. Quant. Spectrosc. Radiat. Transfer*, *37*, 165–182, 1987.

McKeen, S. A., S. C. Liu, and C. S. Kiang, On the chemistry of stratospheric SO_2 from volcanic eruptions, *J. Geophys. Res.*, *89*, 4873–4881, 1984.

McPeters, R. D., The atmospheric SO_2 budget for Pinatubo derived from NOAA-11 SBUV/2 spectral data, *Geophys. Res. Lett.*, *20*, 1971–1974, 1993.

McPeters, R. D., D. F. Heath, and B. M. Schlesinger, Satellite observation of SO_2 from El Chichón: Identification and measurement, *Geophys. Res. Lett.*, *11*, 1203–1206, 1984.

Millan, M. M., Absorption correlation spectrometry, in *Optical Remote Sensing of Air Pollution*, edited by P. Camagni and S. Sandroni, Elsevier Sci., pp. 45–67, New York, 1984.

Newhall, C. G., and S. Self, The volcanic explosivity index (VEI): An estimate of explosive magnitude for historic volcanism, *J. Geophys. Res.*, *87*, 1231–1238, 1982.

Patterson, E. M., Measurements of the imaginary part of the refractive index between 300 and 700 nanometers for Mount St. Helens ash, *Science*, *211*, 836–838, 1981.

Patterson, E. M., and C. O. Pollard, Optical properties of the ash from El Chichon volcano, *Geophys. Res. Lett.*, *10*(4), 317–320, 1983.

Read, W. G., L. Froidevaux, and J. W. Waters, Microwave Limb Sounder (MLS) measurement of SO_2 from Mt. Pinatubo Volcano, *Geophys. Res. Lett.*, *20*, 1299–1302, 1993.

Schnetzler, C. C., G. J. S. Bluth, A. J. Krueger, L. S. Walter, and S. D. Doiron, A sulfur emission index (SEI) for explosive volcanic eruptions (abstract), *Eos Trans. AGU*, *73*(43), Fall Meet. Suppl., 614, 1992.

Self, S., M. R. Rampino, M. S. Newton, and J. A. Wolff, Volcanological study of the great Tamboro eruption of 1815, *Geology*, *12*, 659, 1984.

Sigurdsson, H., Volcanic pollution and climate: The 1783 Laki eruption, *Eos Trans. AGU*, *63*(32), 601–602, 1982.

Stoiber, R. E., and A. Jepsen, Sulfur dioxide contributions to the atmosphere by volcanoes, *Science*, *182*, 577–578, 1973.

Stowe, L. L., R. M. Carey, and P. P. Pellegrino, Monitoring the Mt. Pinatubo aerosol layer with NOAA/11 AVHRR data, *Geophys. Res. Lett.*, *19*, 159–162, 1992.

Wallace, P. J., and T. M. Gerlach, Magmatic vapor source for sulfur dioxide released during volcanic eruptions: Evidence from Mount Pinatubo, *Science*, *265*, 497–499, 1994.

Wu, C. Y. R., and D. L. Judge, SO_2 and CO_2 cross section data in the ultraviolet region, *Geophys. Res. Lett.*, *8*, 769–771, 1981.

P. K. Bhartia, A. J. Krueger, and L. S. Walter, Earth Sciences Directorate, Goddard Space Flight Center, Greenbelt, MD 20771.

G. J. S. Bluth, Department of Geological Engineering and Sciences, Michigan Technological University, Houghton, MI 49931.

N. A. Krotkov, Visiting Scientist Program, USRA, Goddard Space Flight Center, Greenbelt, MD 20771.

C. C. Schnetzler, Department of Geography, University of Maryland, College Park, MD 20742.

I. Sprod, Hughes STX Corporation, 4400 Forbes Boulevard, Lanham, MD 20706.

(Received February 3, 1995; accepted March 29, 1995.)